

Flavour anomalies and dark matter assisted unification in $SO(10)$ GUT

Purushottam Sahu,^{1,*} Aishwarya Bhatta,^{2,†} Rukmani Mohanta,^{2,‡}
Shivaramakrishna Singirala,^{2,§} and Sudhanwa Patra^{1,¶}

¹*Department of Physics, Indian Institute of Technology Bhilai, India*

²*School of Physics, University of Hyderabad, Hyderabad 500046, India*

With the recent experimental hint of new physics from flavor physics anomalies, combined with the evidence from neutrino masses and dark matter, we consider a minimal extension of SM with a scalar leptoquark and a fermion triplet. The scalar leptoquark with couplings to leptons and quarks can explain lepton flavor non-universality observables R_K , $R_{K^{(*)}}$, $R_{D^{(*)}}$ and $R_{J/\psi}$. Neutral component of fermion triplet provides current abundance of dark matter in the Universe. The interesting feature of the proposal is that the minimal addition of these phenomenologically rich particles (scalar leptoquark and fermion triplet) assist in realizing the unification of the gauge couplings associated with the strong and electroweak forces of standard model when embedded in the non-supersymmetric $SO(10)$ grand unified theory. We discuss on unification mass scale and the corresponding proton decay constraints while taking into account the GUT threshold corrections.

*Electronic address: purushottams@iitbhilai.ac.in

†Electronic address: aish.bhatta@gmail.com

‡Electronic address: rmisp@uohyd.ac.in

§Electronic address: krishnas542@gmail.com

¶Electronic address: sudhanwa@iitbhilai.ac.in

I. INTRODUCTION

Standard model of particle physics (SM) beautifully explains the gauge theory of strong, electromagnetic and weak interactions, with all its predictions testified at current experiments including LHC. Still it is known that many observed phenomena like neutrino masses and mixing [1–10], dark matter [11–14], matter anti-matter asymmetry [15–18] and the recent flavor anomalies, see for example [19] and references therein, cannot be addressed within its framework. This motivates to explore other possible beyond standard model (BSM) frameworks which have the potential to address these unsolved issues of the SM. It is believed that the ultimate theory of elementary particles might be an effective low energy approximation of some grand unified theory (GUT) or part of another theory at high scale.

Though most of the flavor observables go along with the SM, there are a collection of recent measurements in semileptonic B meson decays, involving $b \rightarrow s\ell\ell$ ($\ell = e, \mu$) and $b \rightarrow c\bar{\nu}_l$ ($l = \mu, \tau$) quark level transitions, that are incongruous with the SM predictions. The most conspicuous measurements, hinting the physics beyond SM are the lepton flavor universality violating parameters: R_K with a discrepancy of 3.1σ [20–24], $R_{K^{(*)}}$ with a disagreement at the level of $(2.1 - 2.5)\sigma$ [25, 26], $R_{D^{(*)}}$ with 3.08σ discrepancy [27–30] and $R_{J/\psi}$ with a deviation of nearly 2σ [31–33] from their SM predictions. Though the Belle Collaboration [34, 35] has also announced their measurements on $R_{K^{(*)}}$ in various q^2 bins, however these measurements have large uncertainties. Besides the $R_{K^{(*)}}$ parameters, the P'_5 optimized observable disagrees with the SM at the level of 4σ in the $(4.3 - 8.68)$ GeV^2 q^2 -bin [36–38] and the decay rate of $B \rightarrow K^*\mu\mu$ shows 3σ discrepancy [39]. The branching ratio of $B_s \rightarrow \phi\mu\mu$ channel also disagrees with the theory at the level of 3σ [40] in low q^2 .

One of the possible explanation for these flavor anomalies is the existence of leptoquarks (LQ) leading to the transitions $b \rightarrow s\ell\ell$ and $b \rightarrow c\bar{\nu}_l$. It is believed that LQs may lead to interesting new physics searches and could be the next big discovery at LHC. Since, by definition, LQ connecting both leptons and quarks simultaneously may have its origin from quark-lepton symmetry, Pati-Salam symmetry, $SO(10)$ and other grand unified models (GUT). In the present work, we wish to study LQ assisted gauge coupling unification of the fundamental forces described by the SM. In the present work, the idea is to construct a TeV scale extension of SM in order to explain the experimental hints of new physics in recently observed flavor anomalies within the framework of non-supersymmetric $SO(10)$

grand unified theory while simultaneously addressing neutrino mass and dark matter. The important feature of the model is that inclusion of a scalar LQ and a fermion triplet DM at few TeV scale on top of SM leads to successful unification of SM gauge couplings.

In the context of GUT, the popular models are $SU(5)$ [41], $SO(10)$ [18, 42–52] and E_6 [53–61], where many of the unsolved issues of the SM can be addressed. In most of the literature, it is found that all GUTs without any intermediate symmetry breaking and in the absence of supersymmetry, fails to unify the gauge couplings corresponding to three fundamental forces as described by SM. Few attempts were successful in gauge coupling unification by adding extra particles on top of SM spectrum at a higher scale. With this idea, we explore a simplified extension of SM at few TeV scale, which can be successfully embedded in a non-supersymmetric $SO(10)$ GUT. The key feature of the work is that the extra particles, isospin triplet fermion and scalar leptoquark (SLQ) which are originally motivated to unify the gauge couplings, can simultaneously address the dark matter of the Universe and flavor anomalies. While examining the gauge coupling unification it is observed that the unification scale and inverse fine structure constant are in conflict with proton decay prediction. In order to satisfy the proton decay limits, we propose the presence of super heavy particles including scalars, fermions and gauge bosons sitting at GUT scale, which can modify the unification scale and the inverse fine structure constant can be explained through one-loop GUT threshold effects[58, 62–67].

The structure of the paper is as follows. In section-II, a realistic TeV scale extension of SM with scalar LQ, fermionic triplet DM and its embedding in non-supersymmetric $SO(10)$ GUT is proposed. Section-III discusses the implications of GUT threshold corrections to gauge coupling constants and unification mass scale in order to comply with the current bound on proton decay. In section-IV, we comment on fermion masses and mixing including the light neutrino masses via type-I seesaw. Addressing of flavor anomalies with scalar LQ is presented in section-V. Section-VI discusses the role of fermion triplet as DM candidate, which was originally motivated for gauge coupling unification. We conclude our results in section-VII.

II. LEPTOQUARK AND DM ASSISTED GAUGE COUPLING UNIFICATION

It has been established in a number of investigations [68–73] that non-supersymmetric grand unified theories including $SO(10)$ GUT can provide successful gauge coupling unification with either an intermediate symmetry or inclusion of extra particles. At the same time, the inability of SM to explain the non-zero neutrino masses, dark matter and recent flavour anomalies requires to explore possible SM extensions. Combining these two ideas, we wish to consider a minimal extension of SM and examine how the unification of gauge couplings are achieved with the minimal extension of SM with a scalar leptoquark $R_2(3_C, 2_L, 7/6_Y)$ and a fermion triplet $\Sigma(1_C, 3_L, 0_Y)$ around TeV scale by embedding the set up in a non-supersymmetric $SO(10)$ GUT with the following symmetry breaking chain,

$$\begin{aligned} SO(10) &\xrightarrow{M_U} SU(3)_C \otimes SU(2)_L \otimes U(1)_Y \quad (\text{with } R_2, \Sigma) \\ &\xrightarrow{M_I} SU(3)_C \otimes SU(2)_L \otimes U(1)_Y \\ &\xrightarrow{M_Z} SU(3)_C \otimes U(1)_Q . \end{aligned} \quad (1)$$

Instead of introducing an intermediate symmetry between $SO(10)$ and SM, we take an intermediate mass scale (M_I) and two new fields R_2 and Σ are included.

It is also important to note that scalar leptoquarks can arise naturally in grand unified theories like Pati-Salam (PS) model based on the gauge group $SU(4)_C \otimes SU(2)_L \otimes SU(2)_R$ [42, 74]. PS model which was originally motivated for quark lepton mass unification already accommodates all scalar LQs mediating interesting B-meson anomalies while keeping the relevant LQ mass to few TeV scale. The issue with simple SM extension with LQs is that it may lead to proton decay, which requires additional symmetry to stabilize the proton. However, the leptoquarks originated from PS symmetry mediate B-physics anomalies but do not cause proton decay. With this motivation we can also consider other novel symmetry breaking chain as

$$SO(10) \xrightarrow{M_U} G_{422(D)} \xrightarrow{M_I} G_{321} \xrightarrow{M_Z} G_{31} \quad (2)$$

where, the used notations are,

$$\begin{aligned} G_{422} &= SU(4)_C \otimes SU(2)_L \otimes SU(2)_R \\ G_{321} &= SU(3)_C \otimes SU(2)_L \otimes U(1)_Y \\ G_{31} &= SU(3)_C \otimes U(1)_Q . \end{aligned} \quad (3)$$

The first stage of symmetry breaking i.e, $SO(10) \rightarrow G_{422}$ is achieved by giving non-zero vev to G_{422} singlets in 54_H (Case A) or 210_H (Case B) at unification scale M_U . It is to be noted that the vev assignment to singlet $\langle(1, 1, 1)\rangle$ belonging to 54_H is even under D-parity. Therefore D-parity is not broken while the vev assignment of the singlet $\langle(1, 1, 1)\rangle$ belonging to 210_H is odd under D-parity. In the next stage symmetry breaking PS to SM gauge group i.e, $G_{422} \rightarrow G_{321}$ at M_I energy scale is achieved by giving non-zero vev to SM singlet contained in $\Delta_R(\overline{10}_{4c}, 1_{2L}, 3_{2R})$ of 126_H . The final stage of the symmetry breaking $G_{321} \rightarrow G_{31}$ is achieved by the SM Higgs doublet contained in $\phi(1_{4c}, 2_{2L}, 2_{2R})$ of 10_H . Here M_I is the energy scale at which the Pati-Salam symmetry is broken into the SM, which is the mass scale of these Pati-Salam multiplets. All the remaining fields are assumed to be heavy at the unification scale M_U . In order to maintain a complete left-right symmetry for Case-A, we added Pati-Salam multiplets $\Delta_L(\overline{10}_{4c}, 3_{2L}, 1_{2R})$ and $\Sigma_R(\overline{1}_{4c}, 1_{2L}, 3_{2R})$, at M_I . In each energy scale the particle content and the corresponding beta coefficients are given in Table I.

In our analysis, the required non-trivial degrees of freedom with fermion triplet dark matter and a scalar leptoquark at TeV scale can lead to gauge coupling unification. The inclusion of Pati-Salam intermediate symmetry only safeguards from rapid proton decay due to scalar leptoquarks at TeV scale, but does not lead to any significant modification to the unification mass scale and gauge coupling unification.

The known SM fermions plus additional sterile neutrinos are contained in 16_F spinorial representation of $SO(10)$ as follows

$$\begin{aligned}
16_F &= Q_L(3, 2, 1/6) + u_R(3, 1, 2/3) + d_R(3, 1, -1/3) \\
&\quad + L_L(1, 2, -1/2) + e_R(1, 1, -1) + N_R(1, 1, 0) \\
&= 15_F(\text{SM Fermions}) + N_R(\text{sterile neutrino}).
\end{aligned} \tag{4}$$

Thus it is obvious that the 16_F spinorial representation provides unification in the matter sector. The presence of sterile neutrinos in 16_F provides sub-eV scale of neutrino masses via type-I seesaw [75–77] and also explains matter anti-matter asymmetry via leptogenesis[78–97]. The 10_H representation of $SO(10)$ GUT contains SM Higgs field $\phi(1_C, 2_L, 1/2_Y)$ which is essential for electroweak symmetry breaking. The SM gauge bosons including 8 gluons (G_μ^a), three weak gauge bosons W_μ^+, W_μ^-, Z_μ and photon are contained in adjoint representation 45_V of $SO(10)$.

TABLE I: The particles (scalars and fermions) content and the Beta coefficients in the breaking intervals for case A and B. Case A is valid for intermediate PS symmetry with discrete D-parity invariance with the presence of extra fields marked in blue.

Interval	Particle content for case A (B)	Beta coefficients A (B)
Scalars		
$M_I - M_U$	$\phi_1(1, 2, 2), \phi_2(1, 2, 2)$ $R_2(15, 2, 2), \Delta_R(\overline{10}, 1, 3),$ $\Delta_L(10, 3, 1)$ (Case-A)	$[b_{4c}, b_{2L}, b_Y] = \left[\frac{2}{3} \left(\frac{-7}{3} \right), \frac{31}{3} \left(\frac{11}{3} \right), \frac{31}{3} \left(\frac{27}{3} \right) \right]$
Fermions		
	$\Psi_L(4, 2, 1), \Psi_R(\overline{4}, 1, 2)$ $\Sigma_L(1, 3, 1), \Sigma_R(1, 1, 3)$	
Scalars		
$M_Z - M_I$	$H(1, 2, 1/2), R_2(3, 2, 7/6)$	$[b_{3c}, b_{2L}, b_Y] = \left[\frac{-20}{3}, \frac{-4}{3}, \frac{86}{15} \right]$
Fermions		
	$Q_L(3, 2, 1/6), u_R(3, 1, 2/3), d_R(3, 1, -1/3)$ $L_L(1, 2, -1/2), e_R(1, 1, -1)$ $N_R(1, 1, 0), \Sigma(1, 3, 0)$	

The evolution of gauge coupling constants $g_i(\mu)$ ($i = 3_C, 2_L, Y$) using standard renormalization group equations (RGEs) [98] is given by,

$$\mu \frac{\partial g_i}{\partial \mu} = \frac{b_i}{16\pi^2} g_i^3 + \frac{1}{(16\pi^2)^2} \sum_j B_{ij} g_i^3 g_j^2. \quad (5)$$

The solutions can be derived in terms of inverse coupling constant, valid from μ to the intermediate scale M_I (with $M_I > \mu$) as,

$$\frac{1}{\alpha_i(\mu)} = \frac{1}{\alpha_i(M_I)} + \frac{b_i}{2\pi} \ln \left(\frac{M_I}{\mu} \right) + \frac{1}{8\pi^2} \sum_j B_{ij} \int_{\mu}^{M_I} \alpha_j(\mu) \frac{d\mu}{\mu}. \quad (6)$$

Here, $\alpha_i = g_i^2/(4\pi)$ and b_i (B_{ij}) is the one (two)-loop beta coefficients in the mass range $M_Z - M_I$ and $M_I - M_U$ which are presented in Table.II. M_Z stands for electroweak scale, M_I is intermediate scale and M_U represents unification scale.

TABLE II: Beta coefficients at one-loop and two-loop levels.

Mass Range	1-loop level	2-loop level
$M_Z - M_I$	$b_i = (-7, -\frac{19}{6}, \frac{41}{10})$	$B_{ij} = \begin{pmatrix} -26 & \frac{9}{2} & \frac{11}{10} \\ 12 & \frac{35}{6} & \frac{9}{10} \\ \frac{44}{5} & \frac{27}{10} & \frac{199}{50} \end{pmatrix}$
$M_I - M_U$	$b'_i = (\frac{-20}{3}, \frac{-4}{3}, \frac{86}{15})$	$B'_{ij} = \begin{pmatrix} -\frac{56}{3} & \frac{15}{2} & \frac{131}{30} \\ 20 & \frac{86}{3} & \frac{29}{5} \\ \frac{524}{15} & \frac{87}{5} & \frac{3721}{150} \end{pmatrix}$

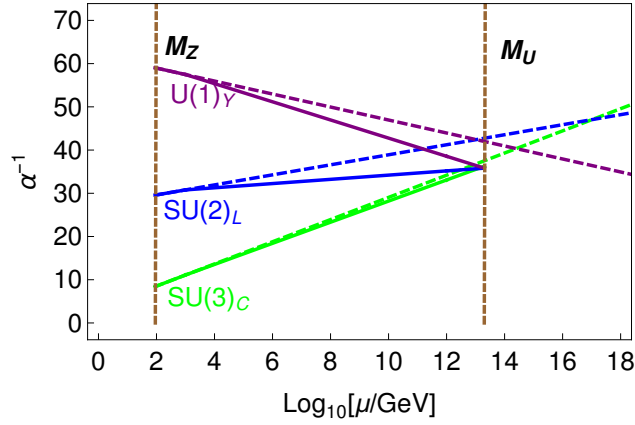


FIG. 1: Evolution of the gauge coupling constants of SM gauge symmetry, where dashed lines are contributions from SM particle content and solid lines correspond to RGEs with SM plus R_2 and Σ . The vertical dotted lines from left-right are representing symmetry breaking scales M_Z as electroweak scale and M_U as unification scale.

We skip the discussion RG evolution of gauge coupling constants with two loop effects. While the one-loop RGEs from mass scale M_Z to M_I and M_I to M_U are read as follows,

$$\begin{aligned} \alpha_i^{-1}(M_Z) &= \alpha_i^{-1}(M_I) + \frac{b_i}{2\pi} \ln \left(\frac{M_I}{M_Z} \right), \\ \alpha_i^{-1}(M_I) &= \alpha_i^{-1}(M_U) + \frac{b'_i}{2\pi} \ln \left(\frac{M_U}{M_I} \right). \end{aligned} \quad (7)$$

Simplifying RGEs, we obtain the analytic solution for unification mass scale as

$$\ln \left(\frac{M_U}{M_Z} \right) = \frac{A_I D_W - B_I D_S}{B_U A_I - B_I A_U}, \quad (8)$$

where, the parameters D_S and D_W are given by

$$D_S = 16\pi \left[\alpha_S^{-1}(M_Z) - \frac{3}{8} \alpha_{\text{em}}^{-1}(M_Z) \right], \quad D_W = 16\pi \left[\sin^2 \theta_W - \frac{3}{8} \right] \alpha_{\text{em}}^{-1}(M_Z). \quad (9)$$

While all other parameters are expressed in terms of one-loop beta coefficients as

$$\begin{aligned} A_I &= \left[\left(8b_{3C} - 3b_{2L} - 5b_Y \right) - \left(8b'_{3C} - 3b'_{2L} - 5b'_Y \right) \right], \quad A_U = \left(8b'_{3C} - 3b'_{2L} - 5b'_Y \right), \\ B_I &= \left[\left(5b_{2L} - 5b_Y \right) - \left(5b'_{2L} - 5b'_Y \right) \right], \quad B_U = \left(5b'_{2L} - 5b'_Y \right). \end{aligned} \quad (10)$$

Using the experimental values of α_{em} , α_S , M_Z and Weinberg mixing angle [99, 100], the estimated values of unification mass scale and inverse GUT coupling constant are given by

$$M_U = 10^{13.27} \text{ GeV and } \alpha_U^{-1} = 36.287. \quad (11)$$

The evolution of gauge couplings for $SU(3)_C$, $SU(2)_L$ and $U(1)_Y$ gauge groups are displayed in Fig.1. Here, the dashed (solid) lines correspond to SM contribution (SM plus R_2 and Σ contributions). The purple line refers to inverse fine structure constant for $U(1)_Y$ group while blue and green lines correspond to $SU(2)_L$ and $SU(3)_C$ groups respectively. It is evident that the SM predictions with dashed lines demonstrate that there is no such gauge coupling unification. However, with the inclusion of extra particles on top of SM at TeV scale, evolution of gauge couplings begin to deviate from the SM results and provide successful gauge coupling unification of weak, electromagnetic and strong forces.

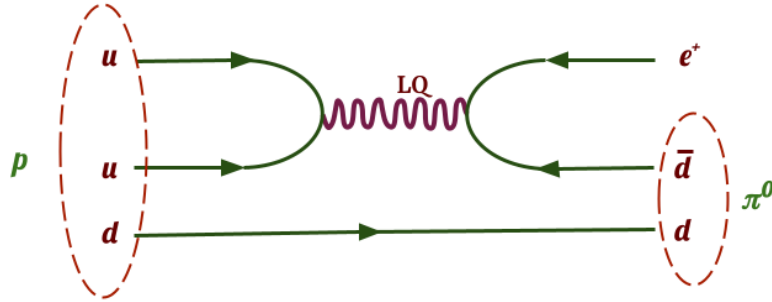


FIG. 2: Proton decay mediated by leptoquark gauge bosons contained in adjoint representation of $SO(10)$.

A. Prediction of proton lifetime

The interesting feature of grand unified theories is that they can have a robust prediction on proton decay with the presence of exotic interactions mediated by super heavy gauge bosons and scalars. Most commonly discussed gauge boson mediated proton decay arises from the covariant derivative of the fermions in 16_F with the gauge bosons contained in 45_V of $SO(10)$, leading to the interaction between quarks and leptons. In our framework, we assume that dominant contributions to proton decay to a neutral pion and a positron comes from the mediation of leptoquark gauge bosons in 45_V . For simplicity, we neglect the contributions from other super heavy particles.

The gauge boson mediated proton life time in the process $p \rightarrow e^+ \pi^0$ [4, 64, 65, 67, 101–106] shown in Fig. 2, is given by

$$\tau_p = \Gamma^{-1}(p \rightarrow \pi^0 e^+) = \frac{64\pi f_\pi^2}{m_p} \left(\frac{M_U^4}{g_U^4} \right) \times \frac{1}{|A_L|^2 |\bar{\alpha}_H|^2 (1 + \mathcal{F} + \mathcal{D})^2 \mathcal{R}}. \quad (12)$$

Here, g_U is the GUT scale coupling related with fine structure constant as $\alpha_U = g_U^2/4\pi$ and the predicted unification mass scale M_U is the typical mass scale of all the super heavy particles. The other parameters, like m_p stands for proton mass, f_π is the pion decay constant \mathcal{R} is the renormalization factor, $\mathcal{R} = (A_{SL}^2 + A_{SR}^2) (1 + |V_{ud}|^2)^2$ with V_{ud} being the CKM-matrix element. Defining $A_R^2 = A_L^2 (A_{SL}^2 + A_{SR}^2)$ and $\alpha_H = \bar{\alpha}_H (1 + \mathcal{F} + \mathcal{D})$, the proton lifetime is modified as follows

$$\tau_{p \rightarrow \pi^0 e^+} = \frac{4}{\pi} \left(\frac{f_\pi^2}{m_p} \right) \left(\frac{M_U^4}{\alpha_U^2} \right) \frac{1}{\alpha_H^2 A_R^2 (1 + |V_{ud}|^2)^2}. \quad (13)$$

In the present model, the long distance enhancement factor is $A_L \simeq 1.25$ while the short distance renormalization factors are $A_{SL} = 2.46$ and $A_{SR} = 2.34$. Using $\alpha_H = 0.012 \text{ GeV}^3$ and the estimated values of M_U and α_U , the proton lifetime is found to be

$$\tau_p = 4.16925 \times 10^{24} \text{ yrs}. \quad (14)$$

This prediction is well below the current bound set by Super-Kamiokande [107] ($\tau_p^{\text{SK}} > 1.6 \times 10^{34} \text{ yrs}$) and Hyper-Kamiokande [108, 109] ($\tau_p^{\text{HK2025}} > 9.0 \times 10^{34} \text{ yrs}$). The gravitational corrections arising from higher dimensional operators or GUT threshold effects can enhance the unification mass scale M_U and the proton lifetime, consistent with the experimental bounds.

In the next section, we will estimate the one-loop GUT threshold contributions to evolution of gauge coupling constants starting from derived unification mass scale M_U . As a result, we get a threshold corrected unification mass scale M_U^{TH} and also examine whether the corrected proton lifetime is in agreement with the experimental constraints.

III. GUT THRESHOLD PREDICTIONS ON UNIFICATION SCALE AND PROTON DECAY

The idea of one-loop GUT threshold corrections is to shift the values of SM gauge couplings at M_U with the presence of super heavy particles. For illustration, let us consider the minimal $SO(10)$ Higgs representation as $10_S \equiv \phi(1, 2, 1/2) + S_1(1, 2, -1/2) + S_2(3, 1, -1/3) + S_3(3, 1, 1/3)$. Since, ϕ is utilized at low scale for electroweak symmetry breaking, all other scalars are considered as super heavy scalars and may contribute to the one-loop GUT threshold corrections. The same argument can be applied to other scalars/fermions/gauge bosons contained in different representation of $SO(10)$ presented in the Table. III.

TABLE III: Super heavy scalars, fermions and vector bosons contributing to the GUT threshold corrections.

	SM	G_{321}
Scalars	10_S	$S_1(\mathbf{1}, \mathbf{2}, -1/2), S_2(\mathbf{3}, \mathbf{1}, -1/3), S_3(\bar{\mathbf{3}}, \mathbf{1}, 1/3)$,
	126_S	$2S_4(\mathbf{3}, \mathbf{1}, -1/3), S_5(\bar{\mathbf{3}}, \mathbf{1}, 1/3), S_6(\mathbf{1}, \mathbf{3}, 1), S_7(\bar{\mathbf{6}}, \mathbf{3}, -1/3)$, $S_8(\mathbf{1}, \mathbf{1}, 0)$ $S_9(\mathbf{1}, \mathbf{1}, -1), S_{10}(\mathbf{1}, \mathbf{1}, -2), S_{11}(\mathbf{3}, \mathbf{1}, 2/3), S_{12}(\mathbf{3}, \mathbf{1}, -4/3), S_{13}(\mathbf{6}, \mathbf{1}, 4/3)$ $S_{14}(\mathbf{6}, \mathbf{1}, 1/3), S_{15}(\mathbf{6}, \mathbf{1}, 2/3), S_{16}(\mathbf{1}, \mathbf{2}, 1/2), S_{17}(\mathbf{1}, \mathbf{2}, -1/2), S_{18}(\mathbf{3}, \mathbf{2}, 1/6)$ $S_{19}(\bar{\mathbf{3}}, \mathbf{2}, -7/6), S_{20}(\bar{\mathbf{3}}, \mathbf{2}, -1/6), S_{21}(\mathbf{8}, \mathbf{2}, 1/2), S_{22}(\mathbf{8}, \mathbf{2}, -1/2), S_{23}(\bar{\mathbf{3}}, \mathbf{3}, 1/3)$
Fermions	16_F	45_F $F_1(\mathbf{1}, \mathbf{1}, 1), 2F_2(\mathbf{1}, \mathbf{1}, 0), F_3(\mathbf{1}, \mathbf{1}, -1), F_4(\mathbf{3}, \mathbf{2}, 1/6), F_5(\mathbf{3}, \mathbf{2}, -5/6)$ $F_6(\bar{\mathbf{3}}, \mathbf{2}, 5/6), F_7(\bar{\mathbf{3}}, \mathbf{2}, -1/6), F_8(\mathbf{3}, \mathbf{1}, 2/3), F_9(\bar{\mathbf{3}}, \mathbf{1}, -2/3), F_{10}(\mathbf{8}, \mathbf{1}, 0)$
Vectors	45_V	$V_1(\mathbf{1}, \mathbf{1}, 1), V_2(\mathbf{1}, \mathbf{1}, 0), V_3(\mathbf{1}, \mathbf{1}, -1), V_4(\mathbf{3}, \mathbf{2}, 1/6), V_5(\mathbf{3}, \mathbf{2}, -5/6)$ $V_6(\bar{\mathbf{3}}, \mathbf{2}, 5/6), V_7(\bar{\mathbf{3}}, \mathbf{2}, -1/6), V_8(\mathbf{3}, \mathbf{1}, 2/3), V_9(\bar{\mathbf{3}}, \mathbf{1}, -2/3)$

A. Analytic formula for threshold corrections

The matching condition at a given symmetry breaking scale μ , by including one-loop GUT threshold corrections is given by [63–67]

$$\alpha_D^{-1}(\mu) = \alpha_P^{-1}(\mu) - \frac{\lambda_D(\mu)}{12\pi}, \quad (15)$$

where $\alpha_P^{-1}(\mu)$ and $\alpha_D^{-1}(\mu)$ denote the inverse coupling constant corresponding to the parent and daughter gauge groups. The parent gauge symmetry gets spontaneously broken down to the daughter gauge group at the mass scale $\mu = M_U$, where, the parent group is a simple $SO(10)$ and the daughter one is a product of different gauge symmetries i.e, $SU(3)_C \times SU(2)_L \times U(1)_Y$. In the present model, the matching conditions for all the inverse gauge couplings of SM at M_U are read as

$$\alpha_i^{-1}(M_U) = \alpha_U^{-1}(M_U) - \frac{\lambda_i(M_U)}{12\pi}. \quad (16)$$

The threshold parameter λ_i is a sum of individual contributions due to the presence of super heavy scalars, fermions and vector bosons (or gauge bosons) with masses M_S , M_F and M_V respectively at GUT scale, is given by

$$\lambda_i(M_U) = \lambda_i^S(M_U) + \lambda_i^F(M_U) + \lambda_i^V(M_U), \quad (17)$$

where,

$$\begin{aligned} \lambda_i^S(M_U) &= \sum_j 2k \text{Tr} \left[t_i^2(S_j) \ln \left(\frac{M_{S_j}}{M_U} \right) \right], \\ \lambda_i^F(M_U) &= \sum_j 8\kappa \text{Tr} \left[t_i^2(F_j) \ln \left(\frac{M_{F_j}}{M_U} \right) \right], \\ \lambda_i^V(M_U) &= \text{Tr} [t_i^2(V_j)] - 21 \sum_j 2k \text{Tr} \left[t_i^2(V_j) \ln \left(\frac{M_{V_j}}{M_U} \right) \right]. \end{aligned} \quad (18)$$

Here t_i represents the generators of the super heavy particles under the i^{th} gauge group. Also the other factors are $k = \frac{1}{2}(1)$ for real (complex) scalars and $\kappa = \frac{1}{2}(1)$ is for Weyl (Dirac) fermions. Now, using the threshold effects in RGEs and after simplifications, one can derive the corrected unification mass scale as follows

$$\begin{aligned} \ln \left(\frac{M_U}{M_Z} \right) &= \frac{A_I D_W - B_I D_S}{B_U A_I - B_I A_U} + \frac{A_I f_B^U - B_I f_A^U}{B_U A_I - B_I A_U} \\ &= \ln \left(\frac{M_U}{M_Z} \right)_{1\text{-loop}} + \Delta \ln \left(\frac{M_U}{M_Z} \right)_{\text{GUT-Th.}}. \end{aligned} \quad (19)$$

First term is the contribution from one-loop RGEs while the second term is for threshold corrections. The one-loop threshold corrections are contained in parameters like f_A^U and f_B^U which depend on λ 's as, $f_A^U = (8\lambda_{3C}^U - 3\lambda_{2L}^U - 5\lambda_Y^U)/6$ and $f_B^U = (5\lambda_{2L}^U - 5\lambda_Y^U)/6$. This simplifies the corrections as

$$\Delta \ln \left(\frac{M_U}{M_Z} \right) = \frac{1}{700} \left[15\lambda_Y^U(M_U) - 13\lambda_{2L}^U(M_U) - 2\lambda_{3C}^U(M_U) \right]. \quad (20)$$

For degenerate masses for super heavy fields:- For the estimation of threshold effects arising from super heavy particles, we assume that all the super heavy gauge bosons have same mass but different from GUT symmetry breaking scale. The same assumption is also applicable to all other super heavy scalars and fermions. The estimated individual threshold corrections are

$$\begin{aligned} \lambda_{3C}^U(M_U) &= 5 - 105\eta_V + 70\eta_S + 64\eta_F, \\ \lambda_{2L}^U(M_U) &= 6 - 126\eta_V + 68\eta_S + 48\eta_F, \\ \lambda_Y^U(M_U) &= 8 - 168\eta_V + \frac{308}{5}\eta_S + 64\eta_F. \end{aligned} \quad (21)$$

Here, $\eta_S = \ln \frac{M_S}{M_U}$, $\eta_F = \ln \frac{M_F}{M_U}$ and $\eta_V = \ln \frac{M_V}{M_U}$. Using these values, the relation for unification mass scale with GUT threshold corrections is modified as,

$$\Delta \ln \left(\frac{M_U}{M_Z} \right) = \frac{1}{175} \left[8 - 168\eta_V - 25\eta_S + 52\eta_F \right]. \quad (22)$$

We have presented few benchmark points in Table. IV for degenerate spectrum of super heavy particles and estimated the unification mass scale and proton lifetime including the threshold effects.

For non-degenerate masses for super heavy vector bosons:- Here, we assume all super heavy color triplet and color singlet gauge bosons are non-degenerate but different from GUT symmetry breaking scale, while other super heavy scalars and fermions are degenerate. With new parameters like η_{V_C} and $\eta_{V_{NC}}$ along with η_S and η_F , the individual threshold corrections are estimated to

$$\begin{aligned} \lambda_{3C}^U(M_U) &= 5 - 21(5\eta_{V_C} + 0\eta_{V_{NC}}) + 70\eta_S + 64\eta_F, \\ \lambda_{2L}^U(M_U) &= 6 - 21(6\eta_{V_C} + 0\eta_{V_{NC}}) + 68\eta_S + 48\eta_F, \\ \lambda_Y^U(M_U) &= 8 - 21 \left(\frac{34}{5}\eta_{V_C} + \frac{6}{5}\eta_{V_{NC}} \right) + \frac{308}{5}\eta_S + 64\eta_F. \end{aligned} \quad (23)$$

$\frac{M_V}{M_U}$	$\frac{M_S}{M_U}$	$\frac{M_F}{M_U}$	λ_{3C}	λ_{2L}	λ_Y	M_U^{TH} [GeV]	τ_p [yrs]
$\frac{1}{500}$	1.5	$\frac{1}{10}$	538.531	706.062	929.631	$10^{15.5598}$	6.88124×10^{33}
$\frac{1}{600}$	2.0	$\frac{1}{10}$	577.811	748.596	977.981	$10^{15.6179}$	1.17508×10^{34}
0.00123	2.03634	0.10048	610.978	787.971	1029.96	$10^{15.7429}$	3.71592×10^{34}
0.00107	1.90066	0.10013	619.977	799.971	1047.96	$10^{15.8025}$	6.43379×10^{34}
0.00060	1.6374	0.0628	640.976	840.969	1106.96	$10^{15.9948}$	3.78152×10^{35}
0.00045	16.989	0.0784	849.969	1047.96	1314.95	$10^{16.0017}$	4.02964×10^{35}

TABLE IV: Numerically estimated values for M_U and τ_p by considering one-loop threshold effects.

where,

$$\eta_S = \ln \frac{M_S}{M_U}, \eta_F = \ln \frac{M_F}{M_U}, \eta_{V_C} = \ln \frac{M_{V_C}}{M_U}, \eta_{V_{NC}} = \ln \frac{M_{V_{NC}}}{M_U}.$$

The notation M_{V_C} and $M_{V_{NC}}$ are the degenerate masses of the vector gauge bosons V_4 to V_9 and V_1 to V_3 respectively (shown in Table. III). Using these input values, GUT threshold corrected unification mass scale is given by

$$\Delta \ln \left(\frac{M_U}{M_Z} \right) = \frac{1}{350} \left[16 - 147 \eta_{V_C} - 189 \eta_{V_{NC}} - 50 \eta_S + 104 \eta_F \right]. \quad (24)$$

$\frac{M_{V_C}}{M_U}$	$\frac{M_{V_{NC}}}{M_U}$	$\frac{M_S}{M_U}$	$\frac{M_F}{M_U}$	λ_{3C}	λ_{2L}	λ_Y	M_U^{TH} [GeV]	τ_p [yrs]
$\frac{1}{400}$	$\frac{1}{100}$	2.0	0.3	617.914	765.08	962.059	$10^{15.287}$	5.57785×10^{32}
$\frac{1}{2500}$	$\frac{1}{100}$	2.5	0.5	846.273	1020.83	1253.36	$10^{15.6519}$	1.60719×10^{34}
$\frac{1}{3000}$	$\frac{1}{300}$	1.5	0.25	785.299	975.796	1231.25	$10^{15.885}$	1.37552×10^{35}
$\frac{1}{4000}$	$\frac{1}{400}$	0.5	0.2	724.324	926.629	1197.63	$10^{16.044}$	5.94931×10^{35}
$\frac{1}{5000}$	$\frac{1}{400}$	0.15	0.2	663.479	872.877	1155.33	$10^{16.16}$	1.73168×10^{36}
$\frac{1}{2000}$	$\frac{1}{500}$	$\frac{1}{2500}$	0.1	108.042	321.143	620.668	$10^{16.323}$	7.77082×10^{36}

TABLE V: Numerically estimated values of M_U and τ_p by including one-loop threshold effects by considering non-degenerate masses for super heavy vector bosons.

In Table V, we have presented various mass values for gauge bosons, scalars and fermions and estimated the threshold corrected unification mass scale and the corresponding proton lifetime. The evolution of gauge coupling constants including one-loop threshold corrections

is shown in Fig. 3 by considering the benchmark given the last row of Table. V. The corresponding corrected unification mass scale and proton lifetime consistent with Super-Kamiokande [107] and Hyper-Kamiokande [108, 109], are

$$M_U^{TH} = 10^{16.323} \text{ GeV}, \quad \tau_p = 7.77082 \times 10^{36} \text{ yrs.} \quad (25)$$

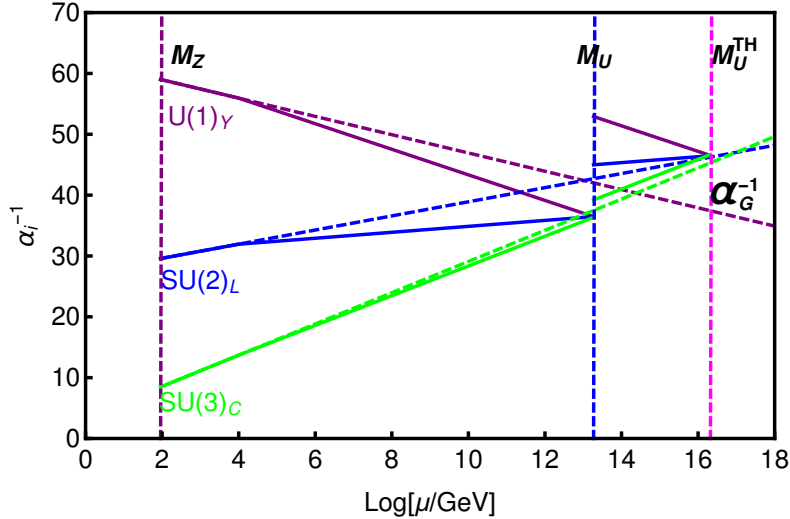


FIG. 3: Unification plot for all three gauge couplings, where the one-loop effects are displayed upto the mass scale M_U while the threshold effects are shown in the mass range $M_U - M_U^{TH}$.

IV. DISCUSSION ON FERMION MASSES AND MIXING

It has been pointed in Witten's work [110] that the minimal non-supersymmetric $SO(10)$ model with only 10_H (containing SM Higgs) and 16_F (accommodating SM fermions plus right-handed neutrinos) predicts $m_d \simeq m_e$, $m_s \simeq m_\mu$, which are ruled out from experiments. In this scenario, the neutrinos have only Dirac masses proportional to up-type quark masses which disagree with the current neutrino oscillation data. Moreover, there is a possibility to have small Majorana masses for right-handed neutrinos via two-loop effects using 16_H on top of 10_H . Thus, the failure of $SO(10)$ model to account correct fermion masses and mixing motivates us to explore all possible non-minimal scenarios.

The correct fermion masses and mixing can be addressed in non-supersymmetric $SO(10)$ theory with the inclusion of extra 10_H [111] while 126_H was introduced for breaking of

Pati-Salam symmetry or left-right symmetry as an intermediate symmetry between $SO(10)$ theory and SM [111–122]. In our present work, we adopt two 10_H and one 126_H representation along with 16_F and 45_F in the fermion sector in order to explain fermion masses and mixing, dark matter and flavor physics anomalies. The SM Higgs can be admixture of two Higgs doublets contained in two 10_H 's and also from 126_H . We assume that Pati-Salam symmetry or left-right symmetry is broken at GUT breaking scale and that is the reason why we are expecting the right-handed neutrinos as well as scalar triplets can have their masses around 10^{13} GeV close to M_U . With this, we have not considered its effects while numerically examining the renormalization evolution equation for gauge couplings.

The $SO(10)$ invariant Yukawa interactions are

$$\mathcal{L}_Y = 16_F^i (Y_{10}^{ij} 10_H + Y_{126}^{ij} \overline{126_H}) 16_F^j + M_{45} 45_F 45_F + \text{h.c.}, \quad (26)$$

where Y_{10} and Y_{126} are complex symmetric matrices. Here, $SO(10)$ or equivalent Pati-Salam symmetry ($SU(4)_C \times SU(2)_L \times SU(2)_R$) is broken down at the predicted unification mass scale $10^{13.27}$ GeV. As a result, since the right-handed symmetry breaking scale is close to M_U , the right-handed neutrinos as well as scalar triplets have their masses around that scale, which can generate neutrino masses and mixing via type-I and type-II seesaw mechanisms respectively.

Using two real representations 10_{H_1} and 10_{H_2} , an equivalent complex 10_H can be constructed as $10_H = 10_{H_1} + i 10_{H_2}$, without effecting the evolution of gauge couplings. Additionally, we introduce a global Pecci-Quinn symmetry forbidding the Yukawa couplings involving 10_H^* [123, 124]. The $U(1)_{PQ}$ transformation of the relevant $SO(10)$ representations are as follows,

$$\begin{aligned} 16_F &\rightarrow e^{i\alpha} 16_F, & 45_F &\rightarrow 45_F, \\ 10_H &\rightarrow e^{-2i\alpha} 10_H, & \overline{126_H} &\rightarrow e^{-2i\alpha} \overline{126_H}. \end{aligned} \quad (27)$$

As a result of this Pecci-Quinn symmetry, we have two separate vevs (vacuum expectation values) $v_{u,d}^{10} \subset 10_H$ and one Yukawa coupling Y_{10} . The other advantage of Pecci-Quinn symmetry [125] is to solve strong CP problem and provide axion dark matter [126–135].

The Yukawa terms for fermion masses and mixing, relevant at the PS symmetry breaking

scale are given by

$$\mathcal{L}_{\text{Yuk}}^{\text{PS}} = Y_{10_F}^{ij} F_L^{iT} \Phi F_R^j + \tilde{Y}_{10_F}^{ij} F_L^{iT} \tilde{\Phi} F_R^j + Y_{126_F}^{ij} F_L^{iT} \bar{\xi} F_R^j + Y_{126_R}^{ij} F_R^{iT} \bar{\Delta}_R F_R^j + M_\Sigma \Sigma_F \Sigma_F + \text{h.c.} \quad (28)$$

The details of mapping of Yukawa couplings at $SO(10)$ and Pati-Salam symmetry can be understood by solving RGEs and interested reader may refer to [136]. Here we consider the vevs v_1 and v_2 from the PS multiplet $(1, 2, 2)$ of 10_H . The primary role of these vevs (of the order of EW scale) is to generate fermion masses and help in breaking of $SU(3)_C \times SU(2)_L \times U(1)_Y$ down to $SU(3)_C \times U(1)_{\text{em}}$. The other vevs are relevant for correcting bad mass relations in fermion masses are $\langle \xi \rangle \approx v_{\xi_1}, v_{\xi_2} \subset 126_H$ in the MeV scale. As pointed out in ref [4], these small induced vevs of Pati-Salam multiplet $(15_{4C}, 2_{2L}, 2_{2R})$ are coming from the important scalar interaction term,

$$V = \lambda_\xi M' 210_H 126_H^\dagger 10_H \supset \lambda_\xi M' (15, 2, 2)_{126} (15, 1, 1)_{210} (1, 2, 2)_{10},$$

This provides the induced vev v_ξ of the neutral component of $\xi(15, 2, 2)$ as,

$$v_\xi = \lambda_\xi M' M_C v_{ew} / M_\xi^2,$$

where, $v_{ew} = \sqrt{v_1^2 + v_2^2}$. Using these vevs and Yukawa couplings, the fermion masses at electroweak scale can be expressed in terms of Yukawa couplings defined at Pati-Salam scale and various vevs arising from 10_H and 126_H are given by

$$\begin{aligned} M_u &\equiv v_u Y_u = v_1 Y_{10_F}^u + v_{\xi_1} Y_{126_F}^u, & M_d &\equiv v_d Y_d = v_2 Y_{10_F}^d + v_{\xi_2} Y_{126_F}^d, \\ M_e &\equiv v_e^{10} Y_e = v_2 Y_{10_F}^e + v_{\xi_2} Y_{126_F}^e, & M_\nu^D &\equiv v_u Y_\nu = v_1 Y_{10_F}^\nu + v_{\xi_1} Y_{126_F}^\nu, \\ M_R &= v_R Y_{126_R}^\nu, & [M_L &= v_L Y_{126_L}^\nu \text{ for } G_{224D}]. \end{aligned} \quad (29)$$

Here, M_u (M_d) denotes the mass matrix for up (down)-type quarks whereas M_e represents the mass matrix of the charged leptons. Also M_ν^D is Dirac neutrino mass matrix, while M_L and M_R stand for Majorana mass matrix for light left-handed and heavy right-handed neutrinos respectively. Applying appropriate boundary condition at Pati-Salam symmetry breaking scale, the simplified fermion mass matrices become [4],

$$\begin{aligned} M_u &= H v_1 + F v_{\xi_1}, & M_d &= H v_2 + F v_{\xi_2} \\ M_\nu^D &= H v_1 - 3F v_{\xi_1}, & M_e &= H v_2 - 3F v_{\xi_2} \\ M_R &= F v_R \end{aligned} \quad (30)$$

Here, H and F are Yukawa coupling matrices derived in terms Yukawa coupling matrices defined at Pati-Salam symmetry. Let us consider a basis where H is real and diagonal. Also define two more parameters; ratio between two Higgs doublet VEVs of 10_H i.e, $r_1 = v_2/v_1$ and ratio between two Higgs doublet VEVs of 126_H i.e, $r_2 = v_{\xi_2}/v_{\xi_1}$. As a result, there are total 13 parameters excluding the VEVs v_R (or v_L) present in the fermion mass fitting: 3 diagonal elements of matrix H , 6 elements of symmetric matrix F , 2 ratios of VEVs r_1, r_2 and two physical phases α and β used in the VEVs. These 13 parameters have been utilised to explain the 13 observables in the charged fermion masses: 9 fermion masses, 3 quark mixing angles and one CP-phase. Also, the resulting Dirac neutrino mass matrix can be expressed in terms of v_R and other input model parameters. So, one can rewrite the simplified fermion mass relations in terms of these ratios of different VEVs as follows [4],

$$\begin{aligned} M_e &= \frac{4r_1r_2}{r_2 - r_1}M_u - \frac{r_1 + 3r_2}{r_2 - r_1}M_d, \\ M_\nu^D &= \frac{3r_1 + r_2}{r_2 - r_1}M_u - \frac{4}{r_2 - r_1}M_d \\ M_R &= \frac{1}{R} \frac{r_1}{r_1 - r_2}M_u - \frac{1}{R} \frac{1}{r_1 - r_2}M_d, \end{aligned} \quad (31)$$

where $R = v_1/v_R$. We can consider a basis where M_u is already diagonal with masses as $M_u = \text{Diag}(m_u, m_c, m_t)$. In this choice of basis, the down-type quark mass matrix can be diagonalised by $\hat{M}_d \simeq V_{\text{CKM}}^\dagger M_d V_{\text{CKM}} = \text{Diag}(m_d, m_s, m_b)$ where V_{CKM} is the usual CKM mixing matrix. It is to be noted that the charged lepton mass matrix can now be fully determined in terms of physical observables of quark sector and two parameters related to ratios of various VEVs i.e, r_1 and r_2 .

Let us consider that the Dirac neutrino mass matrix is approximated to be up-quark mass matrix in the present scenario with the high scale intermediate symmetry as Pati-Salam. Using the seesaw approximation with the mass hierarchy $M_R \gg M_\nu^D \gg M_L$, the resulting light neutrino mass formula via type-I seesaw with the PS symmetry without D-parity as the only intermediate symmetry or type-I+II within D-parity conserving PS symmetry, seesaw contributions are as follows

$$M_\nu = -M_\nu^D M_R^{-1} M_\nu^D \left(+ M_L \quad \text{for } G_{422D} \right). \quad (32)$$

For typical value of $M_R \sim 10^{13.27}$ GeV, $M_\nu^D \sim 100$ GeV, we obtain sub-eV mass for light neutrinos. The out-of-equilibrium decays of right-handed neutrinos can provide the observed

baryon asymmetry of the Universe via type-I leptogenesis. We skip the details of fermion mass fitting and its implications to matter-antimatter asymmetry of the universe which can be looked up in recent works [4, 97].

V. ADDRESSING FLAVOR ANOMALIES WITH SCALAR LEPTOQUARK R_2

It has been already examined that inclusion of TeV scale SLQ and a fermion triplet DM candidate leads to successful unification of the gauge coupling, when embedded in a non-supersymmetric $SO(10)$ GUT. The presence of TeV scale SLQ arising from GUT framework has interesting low-energy phenomenology like explaining flavor anomalies, muon $g - 2$, collider studies etc [137]. However, in the present work, we stick with discussions of phenomenological implications of SLQ to recent flavor anomalies in semileptonic B decays. In recent times, several intriguing deviations at $(2 - 4)\sigma$ significance level, have been realized by the three pioneering experiments: Babar [138, 139], Belle [34, 35, 140–142] and LHCb [20, 21, 25, 31, 36, 39, 40, 143–145], in the form of lepton flavour universality (LFU) violation associated with the charged-current (CC) and neutral-current (NC) transitions in semileptonic B decays. These discrepancies can't be accommodated in the SM and are generally interpreted as smoking-gun signals of NP contributions. The discrepancies in the CC sector are usually attributed to the presence of new physics in $b \rightarrow c\tau\bar{\nu}_\tau$ transition, whereas in the NC sector to $b \rightarrow s\mu\mu$ process. It has been shown in the literature that various leptoquark scenarios can successfully address these anomalies. Here, we will show that $R_2(3, 2, 7/6)$ leptoquark present in our model can successfully explain these discrepancies.

The generalized effective Hamiltonian accountable for the charged-current $b \rightarrow c\tau\bar{\nu}_\ell$ transitions is given as [146]

$$\mathcal{H}_{\text{eff}}^{\text{CC}} = \frac{4G_F}{\sqrt{2}} V_{cb} \left[(\delta_{\ell\tau} + C_{V_1}^\ell) \mathcal{O}_{V_1}^\ell + C_{V_2}^\ell \mathcal{O}_{V_2}^\ell + C_{S_1}^\ell \mathcal{O}_{S_1}^\ell + C_{S_2}^\ell \mathcal{O}_{S_2}^\ell + C_T^\ell \mathcal{O}_T^\ell \right], \quad (33)$$

where G_F and V_{cb} represent the Fermi constant and the Cabibbo-Kobayashi-Maskawa (CKM) matrix element respectively. C_X^ℓ are the new Wilson coefficients, with $X = V_{1,2}, S_{1,2}, T$, which can arise only when NP prevails. The corresponding four-fermion op-

erators \mathcal{O}_X^ℓ can be expressed as

$$\begin{aligned}\mathcal{O}_{V_1}^\ell &= (\bar{c}_L \gamma^\mu b_L) (\bar{\tau}_L \gamma_\mu \nu_{\ell L}), & \mathcal{O}_{V_2}^\ell &= (\bar{c}_R \gamma^\mu b_R) (\bar{\tau}_L \gamma_\mu \nu_{\ell L}), \\ \mathcal{O}_{S_1}^\ell &= (\bar{c}_L b_R) (\bar{\tau}_R \nu_{\ell L}), & \mathcal{O}_{S_2}^\ell &= (\bar{c}_R b_L) (\bar{\tau}_R \nu_{\ell L}), \\ \mathcal{O}_T^\ell &= (\bar{c}_R \sigma^{\mu\nu} b_L) (\bar{\tau}_R \sigma_{\mu\nu} \nu_{\ell L}),\end{aligned}\quad (34)$$

where $f_{L(R)} = P_{L(R)} f$ with $P_{L(R)} = (1 \mp \gamma_5)/2$, represent the chiral fermion fields f .

The effective Hamiltonian delineating the NC transitions $b \rightarrow s \ell^+ \ell^-$ is given as [147, 148]

$$\mathcal{H}_{\text{eff}}^{\text{NC}} = -\frac{4G_F}{\sqrt{2}} V_{tb} V_{ts}^* \left[\sum_{i=1}^6 C_i(\mu) \mathcal{O}_i + \sum_{i=7,9,10,S,P} \left(C_i(\mu) \mathcal{O}_i + C'_i(\mu) \mathcal{O}'_i \right) \right], \quad (35)$$

where $V_{tb} V_{ts}^*$ represents the product of CKM matrix elements, C_i 's denote the Wilson coefficients and \mathcal{O}_i 's are the four-fermion operators expressed as:

$$\begin{aligned}\mathcal{O}_7^{(\prime)} &= \frac{\alpha_{\text{em}}}{4\pi} \left[\bar{s} \sigma_{\mu\nu} \{ m_s P_{L(R)} + m_b P_{R(L)} \} b \right] F^{\mu\nu}, \\ \mathcal{O}_9^{(\prime)} &= \frac{\alpha_{\text{em}}}{4\pi} (\bar{s} \gamma^\mu P_{L(R)} b) (\bar{\ell} \gamma_\mu \ell), & \mathcal{O}_{10}^{(\prime)} &= \frac{\alpha_{\text{em}}}{4\pi} (\bar{s} \gamma^\mu P_{L(R)} b) (\bar{\ell} \gamma_\mu \gamma_5 \ell), \\ \mathcal{O}_S^{(\prime)} &= \frac{\alpha_{\text{em}}}{4\pi} (\bar{s} P_{L(R)} b) (\bar{\ell} \ell), & \mathcal{O}_P^{(\prime)} &= \frac{\alpha_{\text{em}}}{4\pi} (\bar{s} P_{L(R)} b) (\bar{\ell} \gamma_5 \ell).\end{aligned}\quad (36)$$

The primed as well as scalar/pseudoscalar operators are absent in the SM and can be generated only in beyond the SM scenarios.

A. New contributions with scalar leptoquark

In the context of the present model, the flavour sector will be sensitive to the presence of the SLQ $R_2(3, 2, 7/6)$, which can provide additional contributions to the CC mediated $b \rightarrow c \ell \bar{\nu}$ as well as NC $b \rightarrow s \ell^- \ell^+$ processes and can elucidate the observed data reasonably well. The SLQ couples simultaneously to quark and lepton fields through flavor dependent Yukawa couplings and the corresponding interaction Lagrangian can be written as [149, 150],

$$\mathcal{L}_{\text{int}} = \lambda_R^{ij} \bar{Q}_{Li} \ell_{Rj} R_2 - \lambda_L^{ij} \bar{u}_{Ri} R_2 i \tau_2 L_{Lj} + \text{h.c.}, \quad (37)$$

where the couplings $\lambda_{L,R}$ are in general 3×3 complex matrices, $R_2 = \left(R_2^{(5/3)} \ R_2^{(2/3)} \right)^T$, $Q_L(L_L)$ represents the left-handed quark (lepton) doublet, $u_R(\ell_R)$ is the right-handed singlet up-type quark (charged lepton) and the generation indices are characterized by i, j . The

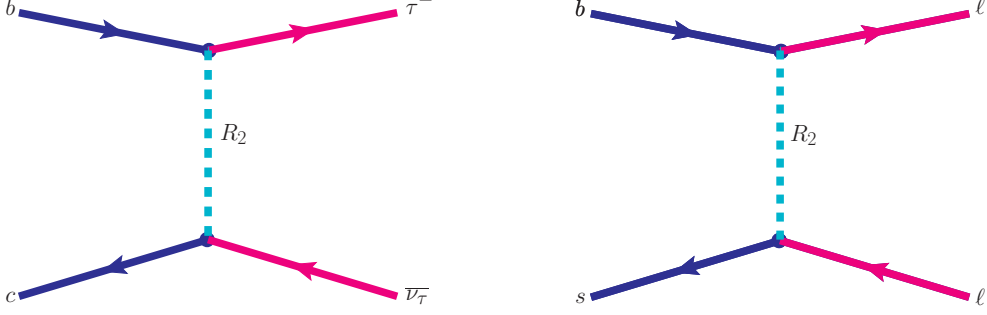


FIG. 4: Feynman diagram for the CC transition $b \rightarrow c\tau^-\bar{\nu}_\tau$ (left panel) and NC process $b \rightarrow s\ell^+\ell^-$ (right panel) induced by the scalar leptoquark $R_2^{(2/3)}$.

interaction Lagrangian (37) in the mass basis can be obtained after the expanding the $SU(2)$ indices as [149]

$$\begin{aligned} \mathcal{L}_{\text{int}} = & (V_{\text{CKM}}\lambda_R)^{ij}\bar{u}_{Li}\ell_{Rj}R_2^{(5/3)} + \lambda_R^{ij}\bar{d}_{Li}\ell_{Rj}R_2^{(2/3)} \\ & + \lambda_L^{ij}\bar{u}_{Ri}\nu_{Lj}R_2^{(2/3)} - \lambda_L^{ij}\bar{u}_{Ri}\ell_{Lj}R_2^{(5/3)} + \text{h.c.} \end{aligned} \quad (38)$$

Here the superscripts on R_2 specify its electric charge and the mass bases for quark doublets are considered as $((V_{\text{CKM}}^\dagger u_L)^i, d_L^i)^T$ while for lepton doublets as $(\nu_L^i, \ell_L^i)^T$, neglecting the mixing in the lepton sector. Thus, from eqn. (38), one can notice that the exchange of $R_2^{(2/3)}$ can induce new contribution to both $b \rightarrow c\tau\bar{\nu}_\tau$ as well as $b \rightarrow s\mu^-\mu^+$ transitions at tree-level as shown in Fig. 4.

For $b \rightarrow c\tau\bar{\nu}_\tau$ it generates additional scalar as well as tensor interactions at the LQ mass scale ($\mu = m_{\text{LQ}}$) as:

$$C_{S_2}^{\text{NP}}(m_{\text{LQ}}) = 4C_T^{\text{NP}}(m_{\text{LQ}}) = \frac{1}{4\sqrt{2}G_F V_{cb}} \frac{\lambda_L^{23}(\lambda_R^{33})^*}{m_{\text{LQ}}^2}, \quad (39)$$

where m_{LQ} represents the leptoquark mass, and we consider a typical TeV scale SLQ in our analysis. It should be noted that the new Wilson coefficients as shown in eqn. (39) rely on the LQ mass scale $\mu(m_{\text{LQ}})$, and hence, it is essential to evolve their values from the m_{LQ} scale to the b -quark mass scale $\mu = m_b$ through the renormalization-group equation (RGE), which are expressed as [151, 152]

$$\begin{pmatrix} C_{S_2}^{\text{NP}}(m_b) \\ C_T^{\text{NP}}(m_b) \end{pmatrix} = \begin{pmatrix} 1.752 & -0.287 \\ -0.004 & 0.842 \end{pmatrix} \begin{pmatrix} C_{S_2}^{\text{NP}}(m_{\text{LQ}}) \\ C_T^{\text{NP}}(m_{\text{LQ}}) \end{pmatrix}. \quad (40)$$

Similarly, after performing the Fierz transformation, the new contribution to the $b \rightarrow s\mu^+\mu^-$ process can be obtained from Eq. (38) as,

$$\mathcal{H}_{\text{LQ}} = \frac{\lambda_R^{32}(\lambda_R^{22})^*}{8m_{\text{LQ}}^2} (\bar{s}\gamma^\mu(1-\gamma_5)b) (\bar{\mu}\gamma_\mu(1+\gamma_5)\mu) \equiv \frac{\lambda_R^{32}(\lambda_R^{22})^*}{4m_{\text{LQ}}^2} (O_9 + O_{10}). \quad (41)$$

Thus, comparing (41) with (35), one can obtain the new Wilson coefficients as

$$C_9^{\text{NP}} = C_{10}^{\text{NP}} = -\frac{\pi}{2\sqrt{2}G_F\alpha_{\text{em}}V_{tb}V_{ts}^*} \frac{\lambda_R^{32}(\lambda_R^{22})^*}{m_{\text{LQ}}^2}. \quad (42)$$

After delineating the additional contributions to the Wilson coefficients for the $b \rightarrow c\tau\bar{\nu}$ and $b \rightarrow s\mu^+\mu^-$ transitions, we now proceed to constrain the new parameters. We perform a global-fit using all the relevant experimental observables to constrain these new couplings. The list of the observables are provided in the following subsection.

B. List of observables used in global-fit

In this analysis, we incorporate the following observables for constraining the new couplings.

1. Observables associated with $b \rightarrow s\mu^+\mu^-$ transitions:

- **R_K and R_{K^*}** : The LFU violating observables R_K and R_{K^*} , expressed as

$$R_K = \frac{\text{BR}(B^+ \rightarrow K^+\mu^+\mu^-)}{\text{BR}(B^+ \rightarrow K^+e^+e^-)}, \quad R_{K^*} = \frac{\text{BR}(B^0 \rightarrow K^{*0}\mu^+\mu^-)}{\text{BR}(B^0 \rightarrow K^{*0}e^+e^-)}. \quad (43)$$

The recently updated values of R_K [22] and R_{K^*} [25], by LHCb experiment in the low q^2 bins are given as:

$$R_K^{\text{LHCb}} = 0.846_{-0.041}^{+0.044}, \quad q^2 \in [1.1, 6] \text{ GeV}^2, \quad (44)$$

$$R_{K^*}^{\text{LHCb}} = \begin{cases} 0.660_{-0.070}^{+0.110} \pm 0.024 & q^2 \in [0.045, 1.1] \text{ GeV}^2, \\ 0.685_{-0.069}^{+0.113} \pm 0.047 & q^2 \in [1.1, 6.0] \text{ GeV}^2. \end{cases} \quad (45)$$

In addition to the LHCb results, the Belle experiment also has recently reported new measurements on R_K [34] and R_{K^*} [35] in several other bins. However, as the Belle results have comparatively larger uncertainties, we do not consider them in our fit for constraining the new parameters.

- $B_s \rightarrow \mu^+ \mu^-$:

The current average value on the branching fraction of $B_s \rightarrow \mu^+ \mu^-$ process from the combined results of ATLAS, CMS and LHCb is [153]:

$$\text{BR}(B_s^0 \rightarrow \mu^+ \mu^-) = (2.69_{-0.35}^{+0.37}) \times 10^{-9}, \quad (46)$$

which has 2.4σ deviation from its SM prediction [154]

$$\text{BR}(B_s^0 \rightarrow \mu^+ \mu^-)^{\text{SM}} = (3.65 \pm 0.23) \times 10^{-9}. \quad (47)$$

- $B \rightarrow K^* \mu \mu$ and $B_s \rightarrow \phi \mu \mu$ processes:

- We consider the following set of angular observables from $B^0 \rightarrow K^{*0} \mu^+ \mu^-$ process: the form factor independent optimized observables $P_{1,2,3}, P'_{4,5,6,8}$, the longitudinal polarization fraction (F_L) and the forward-backward asymmetry (A_{FB}) in the following q^2 bins (in GeV^2): $[0.1, 0.98]$, $[1.1, 2]$, $[2, 3]$, $[3, 4]$, $[4, 5]$, $[5, 6]$ and $[1, 6]$ [37].

- For $B_s \rightarrow \phi \mu^+ \mu^-$ mode, we take into account the longitudinal polarization asymmetry (F_L) and CP averaged observables ($S_{3,4,7}, A_{5,6,8,9}$) in the following three q^2 bins (in GeV^2): $[0.1, 2]$, $[2, 5]$, and $[1, 6]$ [144].

2. $b \rightarrow c \tau \bar{\nu}_\tau$: For the CC transitions $b \rightarrow c \tau \nu$, we incorporate the following observables.

- R_D and R_{D^*} : The lepton non-universality observables R_D and R_{D^*} , defined as

$$R_{D^{(*)}} = \frac{\text{BR}(B \rightarrow D^{(*)} \tau \bar{\nu}_\tau)}{\text{BR}(B \rightarrow D^{(*)} \ell \bar{\nu}_\ell)}, \quad (48)$$

with $\ell = e, \mu$. These observables are measured by BaBar [138, 139] and Belle [140, 141, 155] whereas only R_{D^*} has been measured by LHCb [143, 145]. The present world-average values of these ratios obtained by incorporating the data from all these measurements are [27]:

$$R_D^{\text{exp}} = 0.34 \pm 0.027 \pm 0.013, \quad R_{D^*}^{\text{exp}} = 0.295 \pm 0.011 \pm 0.008, \quad (49)$$

exhibit 3.08σ discrepancy with the corresponding SM results [29, 30]

$$R_D^{\text{SM}} = 0.299 \pm 0.003, \quad R_{D^*}^{\text{SM}} = 0.258 \pm 0.005. \quad (50)$$

- $R_{J/\psi}$: Analogously, in the measurement of $R_{J/\psi}$ [31]

$$R_{J/\psi}^{\text{exp}} = \frac{\text{BR}(B \rightarrow J/\psi \tau \bar{\nu}_\tau)}{\text{BR}(B \rightarrow J/\psi \ell \bar{\nu}_\ell)} = 0.71 \pm 0.17 \pm 0.184, \quad (51)$$

a discrepancy of about 1.7σ has been observed with the corresponding SM prediction [32, 33, 156]

$$R_{J/\psi}^{\text{SM}} = 0.289 \pm 0.01. \quad (52)$$

- $B_c^+ \rightarrow \tau^+ \nu_\tau$: This leptonic decay process has not been observed so far, however, indirect constraints on $\text{BR}(B_c^+ \rightarrow \tau^+ \nu_\tau) \lesssim 30\%$ has been enforced using the lifetime of B_c [157–159].

For the numerical estimation of the SM results of the above-mentioned observables, we use the masses of various particles and the lifetime of B_q mesons from PDG [160]. The SM result for $\text{BR}(B_s \rightarrow \mu^+ \mu^-)$ is taken from Ref. [154]. For evaluating the $B \rightarrow K$ transition form factors we use the light cone sum rule (LCSR) approach [161] and for $B_{(s)} \rightarrow K^*(\phi)$ transitions, we use the form factors from Refs. [162, 163]. The expressions for the decay rates for $B \rightarrow D^{(*)} \ell \nu$ and $B_c \rightarrow J/\psi \ell \nu$ are taken from [150]. The form factors used for processes involving $b \rightarrow c$ transitions are as: $B \rightarrow D$ [164], $B \rightarrow D^*$ [165, 166] and for $B_c \rightarrow J/\psi$ [156]. The B_c meson decay constant is considered as $f_{B_c} = 489$ MeV [167] for computing $\text{BR}(B_c \rightarrow \tau \nu_\tau)$ and its expression is taken from [156].

C. Numerical fits of model parameters

Here, we consider the NP contributions to both neutral current $b \rightarrow s \ell \ell$ as well as charged current $b \rightarrow c \tau \bar{\nu}_\tau$ processes, and constrain the NP couplings by confronting the SM results with their corresponding observed data. In doing so, we perform the χ^2 analysis, wherein we use the following expression for our analysis

$$\chi^2(C_i^{\text{NP}}) = \sum_i \frac{[\mathcal{O}_i^{\text{th}}(C_i^{\text{NP}}) - \mathcal{O}_i^{\text{exp}}]^2}{(\Delta \mathcal{O}_i^{\text{exp}})^2 + (\Delta \mathcal{O}_i^{\text{th}})^2}. \quad (53)$$

Here, $\mathcal{O}_i^{\text{th}}(C_i^{\text{NP}})$ are the theoretically predicted values for different observables used in our fit, which are dependent on the new Wilson coefficients C_i^{NP} and $\Delta \mathcal{O}_i^{\text{th}}$ represent the 1σ uncertainties from theory inputs. $\mathcal{O}_i^{\text{exp}}$ and $\Delta \mathcal{O}_i^{\text{exp}}$ illustrate the corresponding experimental

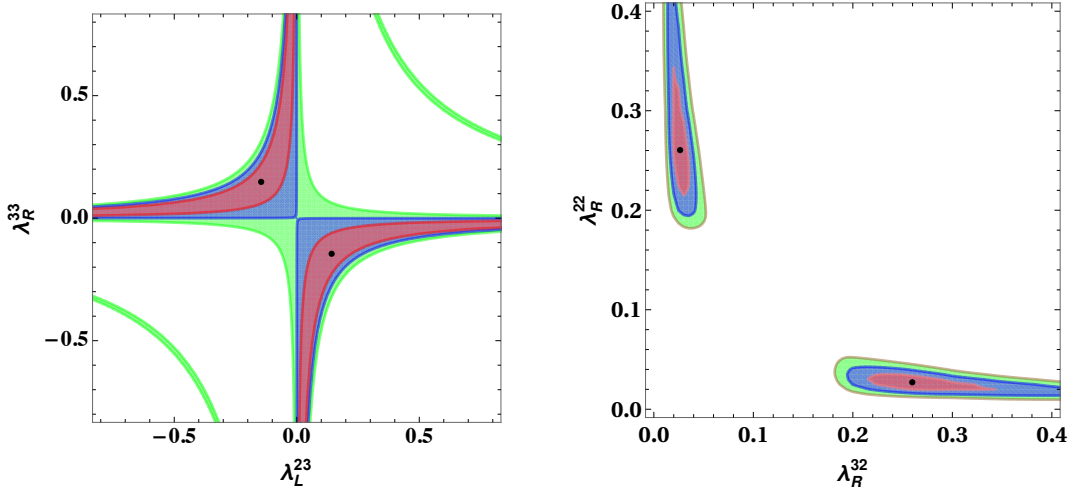


FIG. 5: Constraints on new LQ couplings from observables mediated by $b \rightarrow c\tau\bar{\nu}$ (left panel) and $b \rightarrow s\mu^+\mu^-$ (right panel). Different colors correspond to 1σ , 2σ , and 3σ contours and the black dots represent the best-fit value.

central values and their 1σ uncertainties. In this analysis, we use a representative value of the LQ mass as $m_{\text{LQ}} = 1.2$ TeV, which is congruous with the constraint obtained from LHC experiment [168]. We further take into account the following two scenarios to obtain the best-fit values of the LQ couplings.

- **C-I** : In this case, we include the observables associated with the charged current transitions of leptonic/semileptonic B meson decays, involving only third generation leptons, i.e., the processes mediated through $b \rightarrow c\tau\bar{\nu}_\tau$ transitions
- **C-II** : Here, we incorporate the measurements on leptonic/semileptonic B decay modes involving only second generation leptons, i.e., $b \rightarrow s\mu^+\mu^-$ mediated processes.

In left panel of Fig. 5, we display the constraints on the leptoquark couplings, which are obtained by using the observables associated with $b \rightarrow c\tau\bar{\nu}$ transitions and the plot on the right panel demonstrates the constraints obtained from $b \rightarrow s\mu^-\mu^+$ observables. Different colors in these plots symbolize the 1σ , 2σ , and 3σ contours and the black dots represent the best-fit values. The best-fit values for the LQ couplings obtained for these two cases are presented in Table VI along with their corresponding pull values, defined as:

$$\text{pull} = \sqrt{\chi_{\text{SM}}^2 - \chi_{\text{best-fit}}^2}.$$

Scenarios	Couplings	Best-fit Values	Pull
C-I	$(\lambda_L^{23}, \lambda_R^{33})$	$(-0.143, 0.147)$ $(0.147, -0.143)$	3.5
C-II	$(\lambda_R^{32}, \lambda_R^{22})$	$(0.0265, 0.260)$ $(0.260, 0.0265)$	5.4

TABLE VI: . Best-fit values of new LQ couplings, and pull values for all cases (C-I, C-II).

D. Implications on lepton flavor violating B and τ decays

In this section, we will discuss some of the lepton flavor violating (LFV) decay modes $B_{(s)}$ and Υ mesons as well as τ lepton, due to the impact of the scalar leptoquark, $R_2(\mathbf{3}, \mathbf{2}, 7/6)$. The rare leptonic/semileptonic LFV decays of B mesons involving the quark-level transitions $b \rightarrow s \ell_i^+ \ell_j^-$, occur at tree level via the exchange of the SLQ. For illustration, in the left panel of Fig. 6, we show the Feynman diagram for $b \rightarrow s \tau \mu$ LFV process as a typical example. The effective Hamiltonian for $b \rightarrow s \ell_i^+ \ell_j^-$ process due to the effect of scalar LQ can be given as [169, 170]

$$\mathcal{H}_{\text{eff}}(b \rightarrow s \ell_i^+ \ell_j^-) = \left[G_V (\bar{s} \gamma^\mu P_L b) (\bar{\ell}_i \gamma_\mu \ell_j) + G_A (\bar{s} \gamma^\mu P_L b) (\bar{\ell}_i \gamma_\mu \gamma_5 \ell_j) \right], \quad (54)$$

where the vector and axial vector couplings $G_{V,A}$ are expressed as

$$G_V = G_A = \frac{\lambda_R^{j3} (\lambda_R^{i2})^*}{8m_{\text{LQ}}^2}. \quad (55)$$

This effective Hamiltonian leads to the following decay processes:

1. $B_s \rightarrow \ell_i^+ \ell_j^-$: The branching ratio of the LFV decay process $B_s \rightarrow \ell_i^+ \ell_j^-$, in the presence of scalar LQ is given as [171]

$$\begin{aligned} \text{BR}(\bar{B}_s \rightarrow \ell_i^- \ell_j^+) &= \tau_{B_s} \frac{1}{8\pi M_{B_s}^3} |f_{B_s} G_V|^2 \lambda^{1/2}(M_{B_s}^2, m_i^2, m_j^2) \\ &\times \left[(m_j - m_i)^2 \left(M_{B_s}^2 - (m_i + m_j)^2 \right) + (m_j + m_i)^2 \left(M_{B_s}^2 - (m_i - m_j)^2 \right) \right], \end{aligned} \quad (56)$$

where f_{B_s} represents the decay constant of B_s and

$$\lambda(a, b, c) = a^2 + b^2 + c^2 - 2(ab + bc + ac), \quad (57)$$

is the triangle function.

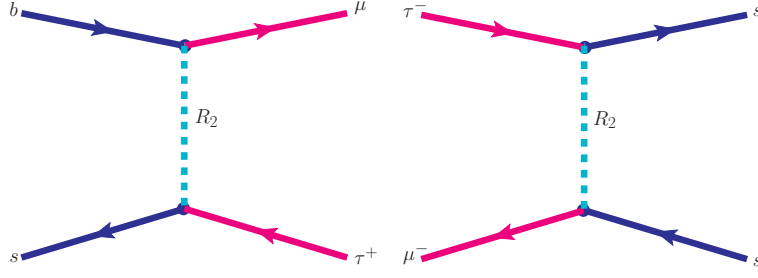


FIG. 6: Feynman diagrams for the LFV processes $b \rightarrow s\tau^+\mu^-$ (left panel), and $\tau \rightarrow \mu\phi$ ($\eta^{(\prime)}$) (right panel) mediated through the exchange of scalar LQ.

2. $\bar{B} \rightarrow \bar{K}\ell_i^+\ell_j^-$: The differential branching fraction of $B \rightarrow K\ell_i^+\ell_j^-$ process is given as [170]

$$\frac{d\text{BR}}{dq^2}(\bar{B} \rightarrow \bar{K}\ell_i^+\ell_j^-) = 2\tau_B \left(a(q^2) + \frac{1}{3}c(q^2) \right), \quad (58)$$

where the coefficients $a(q^2)$ and $c(q^2)$ are expressed as

$$\begin{aligned} a(q^2) = & \Gamma_0 \frac{\sqrt{\lambda_1\lambda_2}}{q^2} f_+^2 \left[(|G_V|^2 + |G_A|^2) \frac{\lambda_1}{4} + |G_S|^2 (q^2 - (m_i + m_j)^2) \right. \\ & + |G_P|^2 (q^2 - (m_i - m_j)^2) + |G_A|^2 M_B^2 (m_i + m_j)^2 + |G_V|^2 M_B^2 (m_i - m_j)^2 \\ & \left. + (M_B^2 - M_K^2 + q^2) \left((m_i + m_j) \text{Re}(G_P G_A^*) + (m_j - m_i) \text{Re}(G_S G_V^*) \right) \right], \quad (59) \end{aligned}$$

$$c(q^2) = -\Gamma_0 f_+^2 \frac{(\lambda_1\lambda_2)^{3/2}}{4q^6} (|G_A|^2 + |G_V|^2), \quad (60)$$

with

$$\Gamma_0 = \frac{1}{2^8 \pi^3 M_B^3}, \quad \lambda_1 = \lambda(M_B^2, M_K^2, q^2), \quad \lambda_2 = \lambda(q^2, m_i^2, m_j^2), \quad (61)$$

and

$$\begin{aligned} G_S &= \frac{1}{2} G_V (m_j - m_i) \left[\frac{M_B^2 - M_K^2}{q^2} \left(\frac{f_0(q^2)}{f_+(q^2)} - 1 \right) - 1 \right], \\ G_P &= \frac{1}{2} G_A (m_i + m_j) \left[\frac{M_B^2 - M_K^2}{q^2} \left(\frac{f_0(q^2)}{f_+(q^2)} - 1 \right) - 1 \right]. \quad (62) \end{aligned}$$

$f_{0,+}$ are the form factors describing $B \rightarrow K$ transitions.

3. $\bar{B} \rightarrow \bar{K}^* \ell_i^+ \ell_j^-$ and $\bar{B}_s \rightarrow \phi \ell_i^+ \ell_j^-$: The differential branching fraction of $\bar{B} \rightarrow \bar{K}^* \ell_i^+ \ell_j^-$ process is given as [170]

$$\begin{aligned}
\frac{d\text{BR}}{dq^2} = & \tau_B \Gamma_V \times \left[A(q^2)^2 \left\{ \frac{2}{3} \lambda_{K^*} \left(1 - \left(\frac{m_i^2}{q^2} \right)^2 \right) + 8M_{K^*}^2 (q^2 - m_i^2) \right. \right. \\
& - \frac{2}{9} \left(1 - \frac{m_i^2}{q^2} \right)^2 \left((M_B^2 - M_{K^*}^2 - q^2)^2 + 8q^2 M_{K^*}^2 \right) \left. \right\} \\
& + B(q^2)^2 \left\{ \frac{\lambda_{K^*}}{6} (M_B^2 - M_{K^*}^2 - q^2)^2 \left(1 - \left(\frac{m_i^2}{q^2} \right)^2 \right) - \frac{\lambda_{K^*}^2}{18} \left(1 - \frac{m_i^2}{q^2} \right)^2 \right. \\
& - \frac{2}{3} \lambda_{K^*} M_{K^*}^2 (q^2 - m_i^2) \left. \right\} + C(q^2)^2 \left\{ \frac{2}{3} \lambda_{K^*} m_i^2 (q^2 - m_i^2) \right\} \\
& - D(q^2)^2 \left\{ \frac{4}{9} \lambda_{K^*} M_{K^*}^2 (q^2 - m_i^2) \left(4 - \frac{m_i^2}{q^2} \right) \right\} \\
& - \text{Re} \left(A(q^2) B(q^2)^* \right) \left\{ \frac{2}{3} \lambda_{K^*} (M_B^2 - M_{K^*}^2 - q^2) \left(1 - \left(\frac{m_i^2}{q^2} \right)^2 - \frac{1}{3} \left(1 - \frac{m_i^2}{q^2} \right)^2 \right) \right\} \\
& - \text{Re} \left(A(q^2) C(q^2)^* \right) \left\{ \frac{4}{3} \lambda_{K^*} m_i^2 \left(1 - \frac{m_i^2}{q^2} \right) \right\} \\
& + \text{Re} \left(B(q^2) C(q^2)^* \right) \left\{ \frac{2}{3} \lambda_{K^*} m_i^2 (M_B^2 - M_{K^*}^2 - q^2) \left(1 - \frac{m_i^2}{q^2} \right) \right\} \left. \right], \quad (63)
\end{aligned}$$

where

$$\Gamma_V = \frac{3\sqrt{\lambda_{K^*}}}{2^{11} M_{K^*}^2 (\pi M_B \beta)^3} |G_V|^2, \quad \lambda_{K^*} = \lambda(M_B^2, M_{K^*}^2, q^2), \quad \beta = \frac{1}{M_{K^*}^2} \lambda^{1/2}(M_B^2, M_{K^*}^2, q^2), \quad (64)$$

and the functions $A(q^2)$, $B(q^2)$, $C(q^2)$ and $D(q^2)$ are related to the various form factors of $B \rightarrow K^*$ transitions as

$$\begin{aligned}
A(q^2) &= (M_B + M_{K^*}) A_1(q^2), & B(q^2) &= \frac{2A_2(q^2)}{(M_B + M_{K^*})}, \\
C(q^2) &= \frac{A_2(q^2)}{(M_B + M_{K^*})} + \frac{2M_{K^*}}{q^2} (A_3(q^2) - A_0(q^2)), & D(q^2) &= \frac{2V(q^2)}{(M_B + M_{K^*})}. \quad (65)
\end{aligned}$$

The same expression can be used for $B_s \rightarrow \phi \ell_i \ell_j$ processes by appropriately replacing the particle masses and the lifetime of B_s meson. For numerical estimation, we use the particle masses and B meson lifetimes as well as other input parameters from PDG [160]. Using $f_{B_s} = (225.6 \pm 1.1 \pm 5.4)$ MeV [172] and best-fit values of the

new couplings from Table VI, we present our predicted results on various branching ratios of LFV decays of B mesons in Table VII. It can be noticed from the table that the branching fractions of various LFV B decays are quite significant in the presence of R_2 scalar leptoquark and are within the reach of Belle-II or LHCb experiments. However, for most of these decays, the experimental limits are not yet available. The LFV channels which have been searched for are $B^+ \rightarrow K^+ \mu^- \tau^+ (\mu^+ \tau^-)$ [173] and $B_s \rightarrow \tau^\pm \mu^\mp$ [174] for which we find our predicted branching fraction values are well below the present 90% CL upper limits. Our obtained result on $\text{BR}(B_s \rightarrow \tau^\pm \mu^\mp)$ is

$$\text{BR}(B_s \rightarrow \tau^\pm \mu^\mp) = \text{BR}(B_s \rightarrow \tau^+ \mu^-) + \text{BR}(B_s \rightarrow \tau^- \mu^+) = 1.3 \times 10^{-9}, \quad (66)$$

which is well below the current experimental limit at 90% C.L. [174] $\text{BR}(B_s \rightarrow \tau^\pm \mu^\mp)^{\text{exp}} < 3.4 \times 10^{-5}$. Our predicted branching ratios for the LFV processes $B_{(s)} \rightarrow (K, K^*, \phi) \mu^- \tau^+ (\mu^+ \tau^-)$ are quite reasonable and are within the reach of Belle-II [175] as well as the upcoming LHCb upgrade [176]. In Fig. 7, we display the differential branching fractions of the decay modes $B^+ \rightarrow K^+ \mu^- \tau^+$ (top-left panel), $B^+ \rightarrow K^{*+} \mu^- \tau^+$ (top-right panel) and $B_s \rightarrow \phi \mu^- \tau^+$ (bottom panel) with respect to q^2 .

4. $\Upsilon(nS) \rightarrow \mu\tau$: The LFV process $\Upsilon(nS) \rightarrow \mu\tau$ can occur at tree level in the LQ model and the corresponding Feynman diagram can be obtained from that of $b \rightarrow s\mu\tau$ process (left panel of Fig. 6) by replacing $s \rightarrow b$, and the branching ratio for this process is given as [178]

$$\text{BR}(\Upsilon(nS) \rightarrow \mu^- \tau^+) = \frac{f_{\Upsilon(nS)}^2 m_{\Upsilon(nS)}^3}{48\pi \Gamma_{\Upsilon(nS)}} \left(2 - \frac{m_\tau^2}{m_{\Upsilon(nS)}^2} - \frac{m_\tau^4}{m_{\Upsilon(nS)}^4} \right) \left(1 - \frac{m_\tau^2}{m_{\Upsilon(nS)}^2} \right) \left| \frac{\lambda_R^{32} \lambda_R^{33*}}{8m_{\text{LQ}}^2} \right|^2. \quad (67)$$

The branching ratio for the process $\Upsilon(nS) \rightarrow \mu^+ \tau^-$ can be obtained from $\text{BR}(\Upsilon(nS) \rightarrow \mu^- \tau^+)$ by appropriately replacing the LQ couplings, i.e., $\lambda_R^{32} \lambda_R^{33*} \rightarrow \lambda_R^{33} \lambda_R^{32*}$. Hence, the branching ratio for $\Upsilon(nS) \rightarrow \mu^\mp \tau^\pm$ process is given as

$$\text{BR}(\Upsilon(nS) \rightarrow \mu^\mp \tau^\pm) = \text{BR}(\Upsilon(nS) \rightarrow \mu^- \tau^+) + \text{BR}(\Upsilon(nS) \rightarrow \mu^+ \tau^-). \quad (68)$$

For numerical estimation, all the particle masses and widths of $\Upsilon(nS)$, $n = 1, 2, 3$ are taken from PDG [160]. The values of $\Upsilon(nS)$ decay constants used are as follows:

Decay modes	Predicted values	Experimental Limit
$B_s \rightarrow \mu^- \tau^+$	3.03×10^{-9}	$< 3.4 \times 10^{-5}$ (90% CL) [174]
$B^+ \rightarrow K^+ \mu^- \tau^+$	1.5×10^{-8}	$< 2.8 \times 10^{-5}$ (90% CL) [173]
$\bar{B}^0 \rightarrow \bar{K}^0 \mu^- \tau^+$	1.4×10^{-8}	...
$B^+ \rightarrow K^{*+} \mu^- \tau^+$	2.91×10^{-8}	...
$\bar{B}^0 \rightarrow \bar{K}^{*0} \mu^- \tau^+$	2.7×10^{-8}	...
$B_s \rightarrow \phi \mu^- \tau^+$	3.5×10^{-8}	...
$B_s \rightarrow \mu^+ \tau^-$	3.2×10^{-9}	$< 3.4 \times 10^{-5}$ (90% CL) [174]
$B^+ \rightarrow K^+ \mu^+ \tau^-$	1.6×10^{-8}	$< 4.5 \times 10^{-5}$ (90% CL) [173]
$\bar{B}^0 \rightarrow \bar{K}^0 \mu^+ \tau^-$	1.5×10^{-8}	...
$B^+ \rightarrow K^{*+} \mu^+ \tau^-$	3.1×10^{-8}	...
$\bar{B}^0 \rightarrow \bar{K}^{*0} \mu^+ \tau^-$	2.8×10^{-8}	...
$B_s \rightarrow \phi \mu^+ \tau^-$	3.7×10^{-8}	...
$\Upsilon(1S) \rightarrow \mu^\mp \tau^\pm$	2.12×10^{-12}	6.0×10^{-6} (95% CL) [160]
$\Upsilon(2S) \rightarrow \mu^\mp \tau^\pm$	2.16×10^{-12}	3.3×10^{-6} (90% CL) [160]
$\Upsilon(3S) \rightarrow \mu^\mp \tau^\pm$	2.82×10^{-12}	3.1×10^{-6} (90% CL) [160]
$\tau^- \rightarrow \mu^- \phi$	4.4×10^{-10}	$< 8.4 \times 10^{-8}$ (90% CL) [177]
$\tau^- \rightarrow \mu^- \eta$	2.18×10^{-10}	$< 6.5 \times 10^{-8}$ (90% CL) [160]
$\tau^- \rightarrow \mu^- \eta'$	5.49×10^{-10}	$< 1.3 \times 10^{-7}$ (90% CL) [160]

TABLE VII: Predicted values of the branching ratios of lepton flavor violating decay channels of B meson and τ lepton in the present model.

$f_{\Upsilon(1S)} = (700 \pm 16)$ MeV, $f_{\Upsilon(2S)} = (496 \pm 21)$ MeV and $f_{\Upsilon(3S)} = (430 \pm 21)$ MeV [178].

With these input parameters the predicted branching ratios of $\Upsilon(nS) \rightarrow \mu^\pm \tau^\mp$ are provided in Table VII, which are far below the current experimental upper limits [160].

5. $\tau \rightarrow \mu \phi$: The Feynman diagram for the LFV decay process $\tau \rightarrow \mu \phi$ is presented in the right panel of Fig. 6 and its branching ratio is expressed as [179]

$$\text{BR}(\tau \rightarrow \mu \phi) = \frac{\tau_\tau f_\phi^2 m_\phi^4}{256 \pi m_\tau^3} \left| \frac{\lambda_R^{23} \lambda_R^{22*}}{m_{\text{LQ}}^2} \right|^2 \times \lambda^{1/2}(m_\phi^2, m_\tau^2, m_\mu^2) \left[-1 + \frac{(m_\mu^2 + m_\tau^2)}{2m_\phi^2} + \frac{(m_\mu^2 - m_\tau^2)^2}{2m_\phi^4} \right], \quad (69)$$

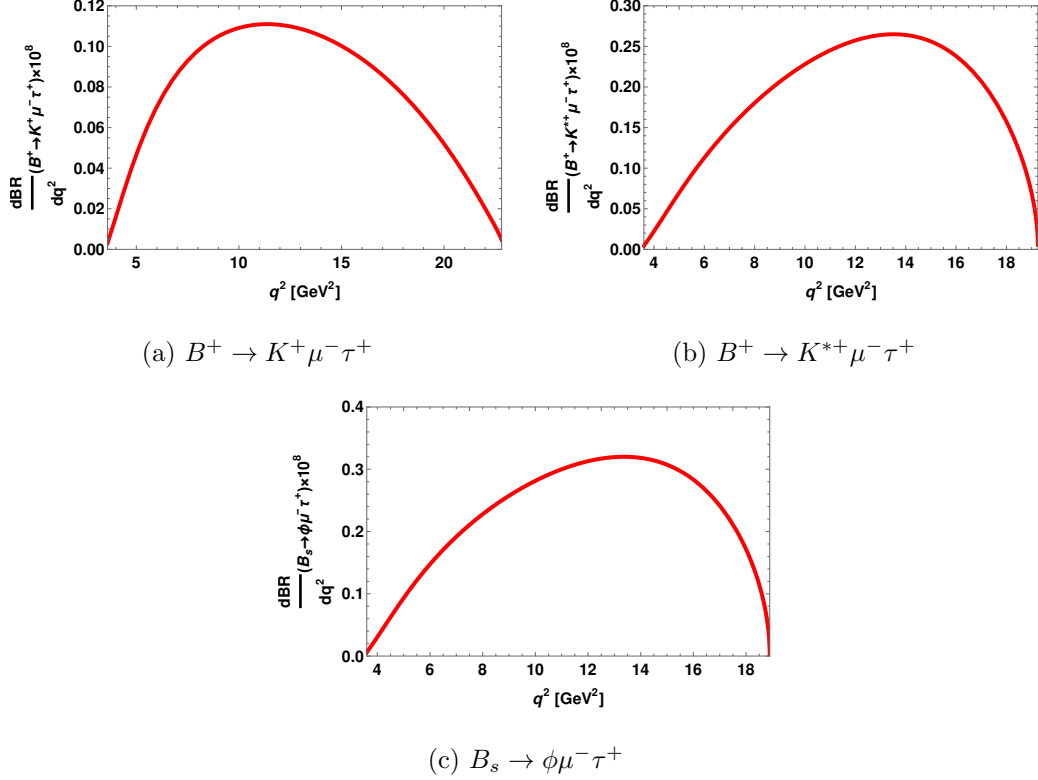


FIG. 7: Behaviour of the differential branching fractions of the LFV processes (a) $B^+ \rightarrow K^+ \mu^- \tau^+$, (b) $B^+ \rightarrow K^{*+} \mu^- \tau^+$ and (c) $B_s \rightarrow \phi \mu^- \tau^+$ with respect to q^2 due to the effect of $R_2^{3/2}$ leptoquark.

where f_ϕ is the ϕ meson decay constant. Using $f_\phi = (238 \pm 3)$ MeV from Ref. [180], and the other input parameters from PDG [160], along with the best-fit values of required new parameters from Table VI, the predicted branching fraction of $\tau \rightarrow \mu \phi$ is shown in Table VII. We find that the branching ratio is substantially enhanced and is within the reach of Belle-II experiment.

6. $\tau \rightarrow \mu \eta^{(\prime)}$: The branching ratio for $\tau \rightarrow \mu \eta^{(\prime)}$ process is given as

$$BR(\tau \rightarrow \mu \eta^{(\prime)}) = \frac{\tau_\tau f_{\eta^{(\prime)}}^2 m_\tau^3}{512\pi} \left| \frac{\lambda_R^{23} \lambda_R^{22*}}{m_{LQ}^2} \right|^2 \left(1 - \frac{m_{\eta^{(\prime)}}^2}{m_\tau^2} \right)^2. \quad (70)$$

Using $f_\eta \simeq -157.63$ MeV, [178], $f_{\eta'} \simeq 31.76$ MeV [178], along with other input parameters from [160] and the best-fit values of LQ couplings from Table VI, our predicted values of branching ratios of $\tau \rightarrow \mu \eta^{(\prime)}$ processes are presented in Table VII, which are found to be substantially lower than the current experimental upper limits.

VI. DARK MATTER

We consider fermion triplet $\Sigma(1, 3, 0)$ coming from the fermion representation 45_F of $SO(10)$. The stability of fermion triplet dark matter is ensured from the matter parity under which 16_F is odd while 45_F is even. SM Higgs is contained in 10_S and the scalar leptoquark R_2 is contained in 126_S , are both even under matter parity [181]. The generic Yukawa term $y\Sigma\bar{\ell}_L\phi$ mediating neutrino masses by type-III seesaw is not allowed, which can be understood as follows. The SM lepton doublet is contained in 16_F , scalar doublet resides in 10_S , while the fermion triplet DM exists in 45_F and the Lagrangian term in $SO(10)$ bilinear $16_F 10_H 45_F$ is actually forbidden because of the matter parity. Hence the fermion triplet mass comes from the invariant bilinear $M_\Sigma 45_F 45_F$ and the relic density of DM is solely controlled by the gauge interactions. The low energy invariant interaction term for fermion triplet DM is given by

$$\mathcal{L}_\Sigma = \frac{i}{2}\text{Tr}[\bar{\Sigma}_R \not{D}\Sigma_R] + \frac{i}{2}\text{Tr}[\bar{\Sigma}_R^c \not{D}\Sigma_R^c] - \left(\frac{1}{2}\text{Tr}[\bar{\Sigma}_R^c M_\Sigma \Sigma_R] + \text{h.c.}\right), \quad (71)$$

where, $\Sigma_R^c = C\bar{\Sigma}_R^T$ is the CP conjugate of Σ_R with C being the operator for charge conjugation and D_μ is the covariant derivative for Σ_R , given by

$$D_\mu = \partial_\mu \Sigma_R + ig \left[\sum_{a=1}^3 \frac{\sigma^a}{2} W_\mu^a, \Sigma_R \right]. \quad (72)$$

Defining the four component Dirac spinor as $\psi^- = \Sigma_R^- + \Sigma_R^{+c}$ and Majorana fermion as $\psi^0 = \Sigma_R^0 + \Sigma_R^{0c}$, we write the Lagrangian for fermion triplet as [182]

$$\begin{aligned} \mathcal{L}_{\text{triplet}} &= \bar{\psi}^- i \not{\partial} \psi^- + \frac{1}{2} \bar{\psi}^0 i \not{\partial} \psi^0 - M_{\psi^-} \bar{\psi}^- \psi^- - \frac{M_{\psi^0}}{2} \bar{\psi}^0 \psi^0 \\ &+ g \left(\cos \theta_w \bar{\psi}^- \gamma_\mu \psi^- Z^\mu + \sin \theta_w \bar{\psi}^- \gamma_\mu \psi^- A^\mu \right) \\ &- g \left(\bar{\psi}^- \gamma^\mu \psi^0 W_\mu^- + \text{h.c.} \right). \end{aligned} \quad (73)$$

A. Relic abundance

The neutral component of fermion triplet (ψ^0) is Majorana type and the charged component (ψ^\pm) is Dirac in nature. At tree-level, both the charged and neutral components remain degenerate in mass. However, one-loop electroweak radiative corrections provide a mass splitting of $\delta = 166$ MeV [183, 184], where $\delta = M_{\psi^\pm} - M_{\psi^0}$. Thus the Majorana fermion ψ^0 is the lightest thermal dark matter candidate in the present model and

its relic density is governed by the gauge interactions [73]. We have used the packages LanHEP [185] and micrOMEGAs [186–188] to extract compute dark matter relic density. With the mentioned mass splitting, co-annihilation's also contribute to dictate relic density in addition to annihilation's. The processes include $\psi^0\bar{\psi}^0 \rightarrow W^+W^-$ (via t-channel ψ^- exchange), $\psi^\pm\psi^\pm \rightarrow W^\pm W^\pm$ (via t-channel ψ^0 exchange), $\psi^+\psi^- \rightarrow f\bar{f}$ (via s-channel A, Z exchange) with $f = u, d, s, c, t, b, e, \mu, \tau$ and $\psi^0\psi^- \rightarrow \bar{f}', f''$ (via s-channel W^- exchange) with $f' = u, c, t, \nu_e, \nu_\mu, \nu_\tau$ and $f'' = d, s, c, e, \mu, \tau$. Fig. 8 depicts the relic density as a function of DM mass, with contribution from the above mentioned channels. The abundance meets the Planck limit (3σ) [189] in the mass region 2.34 TeV to 2.4 TeV [182, 184].

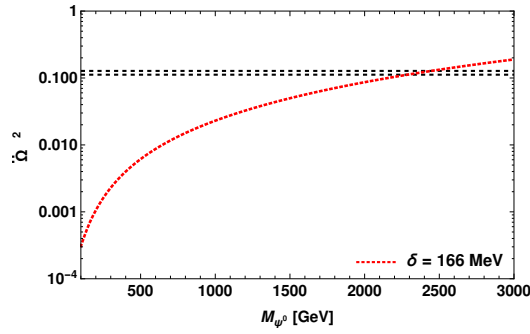


FIG. 8: Relic abundance as a function of DM mass with contributions from annihilation's and co-annihilation's of ψ^0 and ψ_\pm . Black horizontal dashed lines correspond to 3σ region of Planck satellite data.

B. Direct searches

Moving on to the detection perspective, the neutral component ψ^0 can produce a nuclear recoil through Higgs penguin and box diagram with W loop [190]. The effective interaction is given by

$$\mathcal{L} = \sum_i \xi_q^i \bar{\psi}^0 \psi^0 \bar{q}_i q_i. \quad (74)$$

Here,

$$\begin{aligned} \xi_q^i = & -\alpha_2^2 \frac{m_{q_i}}{M_{\psi^0}} \left[-\frac{1 - 4n_W + 3n_W^2 - (4n_W - 2)\log n_W}{m_h^2(1 - n_W)^3} \right. \\ & \left. + \frac{2 - 3n_W + 6n_W^2 - 5n_W^3 + 3n_W(1 + n_W^2)\log n_W}{6m_W^2(1 - n_W)^4} \right], \end{aligned} \quad (75)$$

with $n_W = m_W^2/m_{\psi 0}^2$ and $\alpha_2 = \frac{g^2}{4\pi}$. Thus, the spin-independent (SI) cross section is given by

$$\sigma_{\text{SI}}^{\text{loop}} = \frac{4}{\pi} \mu_r^2 m_p^2 \left(\frac{\xi_q^i}{m_{q_i}} \right)^2 f_p^2, \quad (76)$$

where, m_p is proton mass, μ_r is the reduced mass of DM-nucleon system and $f_p \simeq 0.3$. Figure. 9 projects the SI Cross section as a function of DM mass. We notice that the loop contribution is well below the upper limits levied by PandaX-II [191], XENON1T [192] and LUX [193].

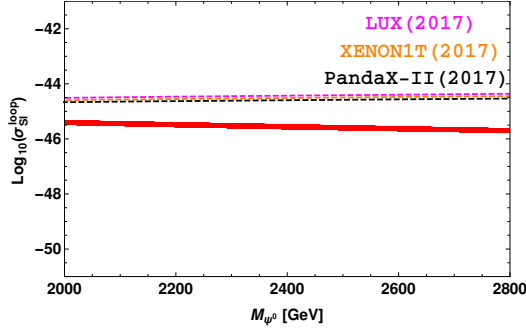


FIG. 9: One-loop SI contribution projected with the stringent upper limits of PandaX-II [191], XENON1T [192] and LUX [193].

In case of indirect searches, DM can provide gamma ray signal via W^\pm at loop level. However, Fermi-LAT with Sommerfeld enhancement rules out such suppressed cross section from a TeV scale DM [194, 195].

VII. CONCLUSION

We have considered an extension of standard model by a scalar leptoquark R_2 and a fermion triplet Σ and embedded the framework in non-SUSY $SO(10)$ GUT. The introduction of R_2 and Σ at few TeV scale assist the unification of gauge couplings of strong and electroweak forces while consistent with flavor anomalies R_K , $R_{K^{(*)}}$, $R_{D^{(*)}}$, $R_{J/\psi}$ and dark matter phenomenology.

The right-handed neutrino which is part of 16_F spinorial representation of $SO(10)$ can explain the non-zero neutrino masses. The dark matter comes from 45_F of $SO(10)$, while the scalar leptoquark is contained in the 126_S . Since 16_F is odd while all other multiplets are even under matter parity P_M and thus ensure the stability of fermion triplet dark matter.

The unification mass scale comes out to be $M_U = 10^{13.27}$ GeV which is well below the limit set by the proton decay experiments. In order to satisfy experimental bound on proton decay, we adopt one loop GUT threshold corrections arising due to presence of super heavy scalars, fermions and gauge bosons by modifying the one-loop beta coefficients and revolution of gauge couplings at the GUT scale M_U . After including threshold corrections, the modified value of unification mass scale is found to be $10^{16.323}$, which resulted the proton life time as $\tau_p = 7.7 \times 10^{36}$ years.

The proposed model incorporates the scalar leptoquark $R_2(3, 2, 7/6)$, which plays a crucial role in explaining the recently observed flavor anomalies in semileptonic B decays. The intriguing feature of this leptoquark is that, it can induce additional contributions to the CC $b \rightarrow c\tau\bar{\nu}_\tau$ as well as NC $b \rightarrow s\ell^+\ell^-$ transitions at the tree level due to the exchange of LQ and hence, can successfully account for the observed discrepancies in the LFU violating observables. In this work, the leptoquark couplings are constrained by using the LFU observables $R_{D^{(*)}}$, $R_{J/\psi}$, $\text{BR}(B_c \rightarrow \tau\bar{\nu}_\tau)$ for $b \rightarrow c\tau\bar{\nu}_\tau$ transitions and $R_{K^{(*)}}$, $\text{BR}(B_s \rightarrow \mu^+\mu^-)$, and various observables of $B \rightarrow K^*\mu^+\mu^-$ and $B_s \rightarrow \phi\mu^+\mu^-$ processes for $b \rightarrow s\ell\ell$ transitions for the representative mass of LQ as $m_{\text{LQ}} = 1.2$ TeV. Using these constrained couplings, we have predicted the branching ratios of various LFV decays of B and B_s mesons such as $B \rightarrow K^{(*)}\ell_i^+\ell_j^-$, $B_s \rightarrow \phi\ell_i^+\ell_j^-$ and $B_s \rightarrow \ell_i^+\ell_j^-$. We found that the branching fractions of these decay modes are substantially enhanced due to the effect of R_2 SLQ and are within the reach of the Belle-II and LHCb experiments. The observation of these decay modes provide an indirect hint for the existence of the SLQ $R_2(3, 2, 7/6)$. In addition, we have also investigated the LFV decays $\Upsilon \rightarrow \mu^\pm\tau^\mp$, $\tau \rightarrow \mu^-\phi$ and $\tau \rightarrow \mu^-\eta(\eta')$. Furthermore, the neutral component of fermion triplet Σ contributes to the relic abundance of the Universe near 2.34 to 2.4 TeV mass regime. One loop spin-independent DM-nucleon cross section is also suitably obtained within upper limits of experiments such as XENON1T, LUX and PandaX-II.

Acknowledgments

SS and RM would like to acknowledge University of Hyderabad IoE project grant no. RC1-20-012. RM acknowledges the support from SERB, Government of India, through grant No. EMR/2017/001448. Purushottam Sahu would like to acknowledge the Ministry

of Education, Govt of India for financial support. PS also acknowledges the support from the Abdus Salam International Centre for Theoretical Physics (ICTP) under the 'ICTP Sandwich Training Educational Programme (STEP)' SMR.3676 .

Appendix A: One loop GUT Threshold corrections to SM gauge couplings

The analytical relation for the threshold corrections at M_{GUT} in the G_{SM} model, are

$$\begin{aligned}\lambda_{3C}^U &= 5 - 21 \left[\eta_{V_4} + \eta_{V_5} + \eta_{V_6} + \eta_{V_7} + \frac{1}{2}\eta_{V_8} + \frac{1}{2}\eta_{V_9} \right] \\ &+ 2 \left[\frac{1}{2}\eta_{S_2} + \frac{1}{2}\eta_{S_3} + \eta_{S_4} + \frac{1}{2}\eta_{S_5} + \frac{15}{2}\eta_{S_7} + \frac{1}{2}\eta_{S_{11}} + \frac{1}{2}\eta_{S_{12}} + \frac{5}{2}\eta_{S_{13}} + \frac{5}{2}\eta_{S_{14}} \right. \\ &+ \left. \frac{5}{2}\eta_{S_{15}} + \eta_{S_{18}} + \eta_{S_{19}} + \eta_{S_{20}} + 6\eta_{S_{21}} + 6\eta_{S_{22}} + \frac{3}{2}\eta_{S_{23}} \right] \\ &+ 8 \left[\eta_{F_4} + \eta_{F_5} + \eta_{F_6} + \eta_{F_7} + \frac{1}{2}\eta_{F_8} + \frac{1}{2}\eta_{F_9} + 3\eta_{F_{10}} \right]\end{aligned}\tag{A1}$$

$$\begin{aligned}\lambda_{2L}^U &= 6 - 21 \left[\frac{3}{2}\eta_{V_4} + \frac{3}{2}\eta_{V_5} + \frac{3}{2}\eta_{V_6} + \frac{3}{2}\eta_{V_7} \right] \\ &+ 2 \left[\frac{1}{2}\eta_{S_1} + 2\eta_{S_6} + 12\eta_{S_7} + \frac{1}{2}\eta_{S_{16}} + \frac{1}{2}\eta_{S_{17}} + \frac{3}{2}\eta_{S_{18}} + \frac{3}{2}\eta_{S_{19}} + \frac{3}{2}\eta_{S_{20}} + 4\eta_{S_{21}} + 4\eta_{S_{22}} + 6\eta_{S_{23}} \right] \\ &+ 8 \left[\frac{3}{2}\eta_{F_4} + \frac{3}{2}\eta_{F_5} + \frac{3}{2}\eta_{F_6} + \frac{3}{2}\eta_{F_7} \right]\end{aligned}\tag{A2}$$

$$\begin{aligned}\lambda_Y^U &= 8 - 21 \left[\frac{3}{5}\eta_{V_1} + \frac{3}{5}\eta_{V_3} + \frac{1}{10}\eta_{V_4} + \frac{5}{2}\eta_{V_5} + \frac{5}{2}\eta_{V_6} + \frac{1}{10}\eta_{V_7} + \frac{4}{5}\eta_{V_8} + \frac{4}{5}\eta_{V_9} \right] \\ &+ 2 \left[\frac{3}{10}\eta_{S_1} + \frac{1}{5}\eta_{S_2} + \frac{1}{5}\eta_{S_3} + \frac{2}{5}\eta_{S_4} + \frac{1}{5}\eta_{S_5} + \frac{9}{5}\eta_{S_6} + \frac{6}{5}\eta_{S_7} + \frac{3}{5}\eta_{S_9} + \frac{12}{5}\eta_{S_{10}} \right. \\ &+ \frac{4}{5}\eta_{S_{11}} + \frac{16}{5}\eta_{S_{12}} + \frac{32}{5}\eta_{S_{13}} + \frac{2}{5}\eta_{S_{14}} + \frac{8}{5}\eta_{S_{15}} + \frac{3}{10}\eta_{S_{16}} + \frac{3}{10}\eta_{S_{17}} + \frac{1}{10}\eta_{S_{18}} \\ &+ \left. \frac{49}{10}\eta_{S_{19}} + \frac{1}{10}\eta_{S_{20}} + \frac{12}{5}\eta_{S_{21}} + \frac{12}{5}\eta_{S_{22}} + \frac{3}{5}\eta_{S_{23}} \right] \\ &+ 8 \left[\frac{3}{5}\eta_{F_1} + \frac{3}{5}\eta_{F_3} + \frac{1}{10}\eta_{F_4} + \frac{5}{2}\eta_{F_5} + \frac{5}{2}\eta_{F_6} + \frac{1}{10}\eta_{F_7} + \frac{4}{5}\eta_{F_8} + \frac{4}{5}\eta_{F_9} \right]\end{aligned}\tag{A3}$$

-
- [1] S. M. Bilenky, in *1999 European School of High-Energy Physics* (1999), pp. 187–217, hep-ph/0001311.
- [2] R. N. Mohapatra and G. Senjanovic, Phys. Rev. Lett. **44**, 912 (1980).
- [3] J. Schechter and J. W. F. Valle, Phys. Rev. D **22**, 2227 (1980).
- [4] K. Babu and R. Mohapatra, Phys. Rev. Lett. **70**, 2845 (1993), hep-ph/9209215.
- [5] J. Hosaka et al. (Super-Kamiokande), Phys. Rev. D **73**, 112001 (2006), hep-ex/0508053.
- [6] Q. R. Ahmad et al. (SNO), Phys. Rev. Lett. **89**, 011301 (2002), nucl-ex/0204008.
- [7] K. Abe et al. (Super-Kamiokande), Phys. Rev. D **94**, 052010 (2016), 1606.07538.
- [8] K. Abe et al. (T2K), Phys. Rev. D **99**, 071103 (2019), 1902.06529.
- [9] F. P. An et al. (Daya Bay), Phys. Rev. Lett. **108**, 171803 (2012), 1203.1669.
- [10] Y. Abe et al. (Double Chooz), Phys. Rev. Lett. **108**, 131801 (2012), 1112.6353.
- [11] F. Zwicky, Astrophys. J. **86**, 217 (1937).
- [12] F. Zwicky, Phys. Rev. **43**, 147 (1933), URL <https://link.aps.org/doi/10.1103/PhysRev.43.147>.
- [13] G. Bertone, D. Hooper, and J. Silk, Phys. Rept. **405**, 279 (2005), hep-ph/0404175.
- [14] Y. Mambrini, N. Nagata, K. A. Olive, J. Quevillon, and J. Zheng, Phys. Rev. D **91**, 095010 (2015), 1502.06929.
- [15] A. Sakharov, Sov. Phys. Usp. **34**, 392 (1991).
- [16] E. W. Kolb and S. Wolfram, Nucl. Phys. B **172**, 224 (1980), [Erratum: Nucl.Phys.B 195, 542 (1982)].
- [17] M. Fukugita and T. Yanagida, Phys. Lett. B **174**, 45 (1986).
- [18] H. Fritzsch and P. Minkowski, Annals Phys. **93**, 193 (1975).
- [19] S. Bifani, S. Descotes-Genon, A. Romero Vidal, and M.-H. Schune, J. Phys. G **46**, 023001 (2019), 1809.06229.
- [20] R. Aaij et al. (LHCb), Phys. Rev. Lett. **113**, 151601 (2014), 1406.6482.
- [21] R. Aaij et al. (LHCb), Phys. Rev. Lett. **122**, 191801 (2019), 1903.09252.
- [22] R. Aaij et al. (LHCb) (2021), 2103.11769.
- [23] C. Bobeth, G. Hiller, and G. Piranishvili, JHEP **12**, 040 (2007), 0709.4174.
- [24] M. Bordone, G. Isidori, and A. Pattori, Eur. Phys. J. **C76**, 440 (2016), 1605.07633.

- [25] R. Aaij et al. (LHCb), JHEP **08**, 055 (2017), 1705.05802.
- [26] B. Capdevila, A. Crivellin, S. Descotes-Genon, J. Matias, and J. Virto, JHEP **01**, 093 (2018), 1704.05340.
- [27] Y. S. Amhis et al. (HFLAV), Eur. Phys. J. C **81**, 226 (2021), 1909.12524.
- [28] H. Na, C. M. Bouchard, G. P. Lepage, C. Monahan, and J. Shigemitsu (HPQCD), Phys. Rev. D **92**, 054510 (2015), [Erratum: Phys.Rev.D 93, 119906 (2016)], 1505.03925.
- [29] S. Fajfer, J. F. Kamenik, and I. Nisandzic, Phys. Rev. **D85**, 094025 (2012), 1203.2654.
- [30] S. Fajfer, J. F. Kamenik, I. Nisandzic, and J. Zupan, Phys. Rev. Lett. **109**, 161801 (2012), 1206.1872.
- [31] R. Aaij et al. (LHCb), Phys. Rev. Lett. **120**, 121801 (2018), 1711.05623.
- [32] W.-F. Wang, Y.-Y. Fan, and Z.-J. Xiao, Chin. Phys. **C37**, 093102 (2013), 1212.5903.
- [33] M. A. Ivanov, J. G. Korner, and P. Santorelli, Phys. Rev. **D71**, 094006 (2005), [Erratum: Phys. Rev.D75,019901(2007)], hep-ph/0501051.
- [34] A. Abdesselam et al. (Belle), JHEP **03**, 105 (2021), 1908.01848.
- [35] A. Abdesselam et al. (Belle) (2019), 1904.02440.
- [36] R. Aaij et al. (LHCb), Phys. Rev. Lett. **111**, 191801 (2013), 1308.1707.
- [37] R. Aaij et al. (LHCb), JHEP **02**, 104 (2016), 1512.04442.
- [38] A. Abdesselam et al. (Belle), in *LHC Ski 2016: A First Discussion of 13 TeV Results* (2016), 1604.04042.
- [39] R. Aaij et al. (LHCb), JHEP **06**, 133 (2014), 1403.8044.
- [40] R. Aaij et al. (LHCb), JHEP **07**, 084 (2013), 1305.2168.
- [41] H. Georgi and S. L. Glashow, Phys. Rev. Lett. **32**, 438 (1974).
- [42] J. C. Pati and A. Salam, Phys. Rev. **D10**, 275 (1974), [Erratum: Phys. Rev.D11,703(1975)].
- [43] L. Lavoura and L. Wolfenstein, Phys. Rev. D **48**, 264 (1993), URL <https://link.aps.org/doi/10.1103/PhysRevD.48.264>.
- [44] G. Senjanović and R. N. Mohapatra, Phys.Rev. **D12**, 1502 (1975).
- [45] T. E. Clark, T.-K. Kuo, and N. Nakagawa, Phys. Lett. **115B**, 26 (1982).
- [46] G. Altarelli and D. Meloni, JHEP **08**, 021 (2013), 1305.1001.
- [47] A. Dueck and W. Rodejohann, JHEP **09**, 024 (2013), 1306.4468.
- [48] D. Meloni, T. Ohlsson, and S. Riad, JHEP **12**, 052 (2014), 1409.3730.
- [49] D. Meloni, T. Ohlsson, and S. Riad, JHEP **03**, 045 (2017), 1612.07973.

- [50] A. Preda, G. Senjanovic, and M. Zantedeschi (2022), 2201.02785.
- [51] J. Chakraborty, R. Maji, S. K. Patra, T. Srivastava, and S. Mohanty, Phys. Rev. D **97**, 095010 (2018), 1711.11391.
- [52] T. Bandyopadhyay and A. Raychaudhuri, Phys. Lett. B **771**, 206 (2017), 1703.08125.
- [53] F. Gursey, P. Ramond, and P. Sikivie, Phys. Lett. **60B**, 177 (1976).
- [54] Q. Shafi, Phys. Lett. B **79**, 301 (1978).
- [55] S. Nandi and U. Sarkar, Phys. Rev. Lett. **56**, 564 (1986).
- [56] B. Stech and Z. Tavartkiladze, Phys. Rev. D **70**, 035002 (2004), hep-ph/0311161.
- [57] C.-S. Huang, Mod. Phys. Lett. A **29**, 1450150 (2014), 1402.2737.
- [58] C. Dash, S. Mishra, S. Patra, and P. Sahu, Nucl. Phys. B **962**, 115239 (2021), 2004.14188.
- [59] C. Dash, S. Mishra, and S. Patra, Phys. Rev. D **101**, 5 (2020), 1911.11528.
- [60] C. Dash, S. Mishra, S. Patra, and P. Sahu (2021), 2109.12536.
- [61] T. Bandyopadhyay and R. Maji (2019), 1911.13298.
- [62] R. N. Mohapatra, Phys. Lett. B **285**, 235 (1992).
- [63] L. J. Hall, Nucl. Phys. **B178**, 75 (1981).
- [64] K. Babu and S. Khan, Phys. Rev. D **92**, 075018 (2015), 1507.06712.
- [65] M. Parida, B. P. Nayak, R. Satpathy, and R. L. Awasthi, JHEP **04**, 075 (2017), 1608.03956.
- [66] J. Schwichtenberg, Eur. Phys. J. C **79**, 351 (2019), 1808.10329.
- [67] J. Chakraborty, R. Maji, and S. F. King, Phys. Rev. D **99**, 095008 (2019), 1901.05867.
- [68] T. FUKUYAMA, International Journal of Modern Physics A **28**, 1330008 (2013), ISSN 1793-656X, URL <http://dx.doi.org/10.1142/S0217751X13300081>.
- [69] M. Frigerio, J. Serra, and A. Varagnolo, JHEP **06**, 029 (2011), 1103.2997.
- [70] R. Alonso, H.-M. Chang, E. E. Jenkins, A. V. Manohar, and B. Shotwell, Phys. Lett. B **734**, 302 (2014), 1405.0486.
- [71] I. Dorsner, J. Drobnak, S. Fajfer, J. F. Kamenik, and N. Kosnik, JHEP **11**, 002 (2011), 1107.5393.
- [72] D. Chang, R. N. Mohapatra, J. Gipson, R. E. Marshak, and M. K. Parida, Phys. Rev. D **31**, 1718 (1985).
- [73] S. Bertolini, L. Di Luzio, and M. Malinský, Physical Review D **80** (2009), ISSN 1550-2368, URL <http://dx.doi.org/10.1103/PhysRevD.80.015013>.
- [74] J. C. Pati and A. Salam, Phys. Rev. D **8**, 1240 (1973).

- [75] P. Minkowski, *Int. J. Mod. Phys. A* **30**, 1530043 (2015).
- [76] T. Ohlsson and M. Pernow, *JHEP* **06**, 085 (2019), 1903.08241.
- [77] E. K. Akhmedov, M. Frigerio, and A. Y. Smirnov, *JHEP* **09**, 021 (2003), hep-ph/0305322.
- [78] C. S. Fong, D. Meloni, A. Meroni, and E. Nardi, *JHEP* **01**, 111 (2015), 1412.4776.
- [79] P. Di Bari, *Prog. Part. Nucl. Phys.* **122**, 103913 (2022), 2107.13750.
- [80] D. Bodeker and W. Buchmuller, *Rev. Mod. Phys.* **93**, 035004 (2021), 2009.07294.
- [81] Z.-z. Xing and Z.-h. Zhao, *Rept. Prog. Phys.* **84**, 066201 (2021), 2008.12090.
- [82] W. Buchmuller and M. Plumacher, *Phys. Lett. B* **389**, 73 (1996), hep-ph/9608308.
- [83] E. Nezri and J. Orloff, *JHEP* **04**, 020 (2003), hep-ph/0004227.
- [84] F. Buccella, D. Falcone, and F. Tramontano, *Phys. Lett. B* **524**, 241 (2002), hep-ph/0108172.
- [85] G. C. Branco, R. Gonzalez Felipe, F. R. Joaquim, and M. N. Rebelo, *Nucl. Phys. B* **640**, 202 (2002), hep-ph/0202030.
- [86] P. Di Bari and A. Riotto, *Phys. Lett. B* **671**, 462 (2009), 0809.2285.
- [87] P. Di Bari and A. Riotto, *JCAP* **04**, 037 (2011), 1012.2343.
- [88] F. Buccella, D. Falcone, C. S. Fong, E. Nardi, and G. Ricciardi, *Phys. Rev. D* **86**, 035012 (2012), 1203.0829.
- [89] P. Di Bari, L. Marzola, and M. Re Fiorentin, *Nucl. Phys. B* **893**, 122 (2015), 1411.5478.
- [90] P. Di Bari and S. F. King, *JCAP* **10**, 008 (2015), 1507.06431.
- [91] P. Di Bari and M. Re Fiorentin, *JHEP* **10**, 029 (2017), 1705.01935.
- [92] P. Di Bari and R. Samanta, *JHEP* **08**, 124 (2020), 2005.03057.
- [93] O. Vives, *Phys. Rev. D* **73**, 073006 (2006), hep-ph/0512160.
- [94] P. Di Bari, *Nucl. Phys. B* **727**, 318 (2005), hep-ph/0502082.
- [95] A. Abada, S. Davidson, F.-X. Josse-Michaux, M. Losada, and A. Riotto, *JCAP* **04**, 004 (2006), hep-ph/0601083.
- [96] A. Abada, S. Davidson, A. Ibarra, F. X. Josse-Michaux, M. Losada, and A. Riotto, *JHEP* **09**, 010 (2006), hep-ph/0605281.
- [97] V. S. Mummidi and K. M. Patel, *JHEP* **12**, 042 (2021), 2109.04050.
- [98] H. Georgi, H. R. Quinn, and S. Weinberg, *Phys. Rev. Lett.* **33**, 451 (1974).
- [99] K. A. Olive et al. (Particle Data Group), *Chin. Phys. C* **38**, 090001 (2014).
- [100] Q. Mou and S. Zheng (2017), 1703.00343.
- [101] S. Bertolini, L. Di Luzio, and M. Malinsky, *Phys. Rev. D* **87**, 085020 (2013), 1302.3401.

- [102] H. Kolesová and M. Malinský, Phys. Rev. D **90**, 115001 (2014), 1409.4961.
- [103] D. Meloni, T. Ohlsson, and M. Pernow (2019), 1911.11411.
- [104] L. E. Ibanez and C. Munoz, Nucl. Phys. B **245**, 425 (1984).
- [105] A. Buras, J. R. Ellis, M. Gaillard, and D. V. Nanopoulos, Nucl. Phys. B **135**, 66 (1978).
- [106] P. Bhupal Dev and R. Mohapatra, Phys. Rev. D **82**, 035014 (2010), 1003.6102.
- [107] K. Abe et al. (Super-Kamiokande), Phys. Rev. D **95**, 012004 (2017), 1610.03597.
- [108] K. Abe et al. (2011), 1109.3262.
- [109] M. Yokoyama (Hyper-Kamiokande Proto), in *Prospects in Neutrino Physics* (2017), 1705.00306.
- [110] E. Witten, Phys. Lett. B **91**, 81 (1980).
- [111] B. Bajc, A. Melfo, G. Senjanovic, and F. Vissani, Phys. Rev. D **73**, 055001 (2006), hep-ph/0510139.
- [112] K. S. Babu and E. Ma, Phys. Rev. D **31**, 2316 (1985), URL <https://link.aps.org/doi/10.1103/PhysRevD.31.2316>.
- [113] G. Anastaze, J. P. Derendinger, and F. Buccella, Z. Phys. C **20**, 269 (1983).
- [114] M. Yasue, Phys. Lett. B **103**, 33 (1981).
- [115] M. Yasue, Phys. Rev. D **24**, 1005 (1981).
- [116] S. Bertolini, L. Di Luzio, and M. Malinsky, Phys. Rev. D **80**, 015013 (2009), 0903.4049.
- [117] S. Bertolini, L. Di Luzio, and M. Malinsky, Phys. Rev. D **81**, 035015 (2010), 0912.1796.
- [118] G. Altarelli and D. Meloni, Journal of High Energy Physics **2013** (2013), ISSN 1029-8479, URL [http://dx.doi.org/10.1007/JHEP08\(2013\)021](http://dx.doi.org/10.1007/JHEP08(2013)021).
- [119] A. Dueck and W. Rodejohann, Journal of High Energy Physics **2013** (2013), ISSN 1029-8479, URL [http://dx.doi.org/10.1007/JHEP09\(2013\)024](http://dx.doi.org/10.1007/JHEP09(2013)024).
- [120] A. S. Joshipura and K. M. Patel, Phys. Rev. D **83**, 095002 (2011), 1102.5148.
- [121] K. S. Babu, B. Bajc, and S. Saad, JHEP **02**, 136 (2017), 1612.04329.
- [122] T. Ohlsson and M. Pernow, JHEP **11**, 028 (2018), 1804.04560.
- [123] R. D. Peccei and H. R. Quinn, Phys. Rev. Lett. **38**, 1440 (1977), URL <https://link.aps.org/doi/10.1103/PhysRevLett.38.1440>.
- [124] R. D. Peccei and H. R. Quinn, Phys. Rev. D **16**, 1791 (1977), URL <https://link.aps.org/doi/10.1103/PhysRevD.16.1791>.
- [125] S. M. Boucenna, T. Ohlsson, and M. Pernow, Phys. Lett. B **792**, 251 (2019), [Erratum:

- Phys.Lett.B 797, 134902 (2019)], 1812.10548.
- [126] R. N. Mohapatra and G. Senjanovic, Z. Phys. C **17**, 53 (1983).
 - [127] D. J. E. Marsh, Phys. Rept. **643**, 1 (2016), 1510.07633.
 - [128] Q. Shafi and F. W. Stecker, Phys. Rev. Lett. **53**, 1292 (1984), URL <https://link.aps.org/doi/10.1103/PhysRevLett.53.1292>.
 - [129] K. S. Jeong, K. Matsukawa, S. Nakagawa, and F. Takahashi (2022), 2201.00681.
 - [130] S. Weinberg, Phys. Rev. Lett. **40**, 223 (1978), URL <https://link.aps.org/doi/10.1103/PhysRevLett.40.223>.
 - [131] F. Wilczek, Phys. Rev. Lett. **40**, 279 (1978), URL <https://link.aps.org/doi/10.1103/PhysRevLett.40.279>.
 - [132] A. Ringwald, Phys. Dark Univ. **1**, 116 (2012), 1210.5081.
 - [133] P. W. Graham, I. G. Irastorza, S. K. Lamoreaux, A. Lindner, and K. A. van Bibber, Ann. Rev. Nucl. Part. Sci. **65**, 485 (2015), 1602.00039.
 - [134] P. Arias, D. Cadamuro, M. Goodsell, J. Jaeckel, J. Redondo, and A. Ringwald, JCAP **06**, 013 (2012), 1201.5902.
 - [135] P. Langacker, R. D. Peccei, and T. Yanagida, Mod. Phys. Lett. A **1**, 541 (1986).
 - [136] T. Ohlsson and M. Pernow, JHEP **09**, 111 (2021), 2107.08771.
 - [137] K. S. Babu, P. S. B. Dev, S. Jana, and A. Thapa, JHEP **03**, 179 (2021), 2009.01771.
 - [138] J. P. Lees et al. (BaBar), Phys. Rev. Lett. **109**, 101802 (2012), 1205.5442.
 - [139] J. P. Lees et al. (BaBar), Phys. Rev. **D88**, 072012 (2013), 1303.0571.
 - [140] M. Huschle et al. (Belle), Phys. Rev. **D92**, 072014 (2015), 1507.03233.
 - [141] S. Hirose et al. (Belle), Phys. Rev. Lett. **118**, 211801 (2017), 1612.00529.
 - [142] A. Abdesselam et al. (Belle) (2019), 1904.08794.
 - [143] R. Aaij et al. (LHCb), Phys. Rev. Lett. **115**, 111803 (2015), [Erratum: Phys. Rev. Lett.115,no.15,159901(2015)], 1506.08614.
 - [144] R. Aaij et al. (LHCb), JHEP **09**, 179 (2015), 1506.08777.
 - [145] R. Aaij et al. (LHCb), Phys. Rev. Lett. **120**, 171802 (2018), 1708.08856.
 - [146] M. Tanaka and R. Watanabe, Phys. Rev. **D87**, 034028 (2013), 1212.1878.
 - [147] M. Misiak, Nucl. Phys. **B393**, 23 (1993), [Erratum: Nucl. Phys.B439,461(1995)].
 - [148] A. J. Buras and M. Munz, Phys. Rev. **D52**, 186 (1995), hep-ph/9501281.
 - [149] S. Iguro, T. Kitahara, Y. Omura, R. Watanabe, and K. Yamamoto, JHEP **02**, 194 (2019),

1811.08899.

- [150] Y. Sakaki, M. Tanaka, A. Tayduganov, and R. Watanabe, Phys. Rev. **D88**, 094012 (2013), 1309.0301.
- [151] M. Blanke, A. Crivellin, S. de Boer, T. Kitahara, M. Moscati, U. Nierste, and I. Nišandžić, Phys. Rev. D **99**, 075006 (2019), 1811.09603.
- [152] M. González-Alonso, J. Martin Camalich, and K. Mimouni, Phys. Lett. B **772**, 777 (2017), 1706.00410.
- [153] (2020).
- [154] C. Bobeth, M. Gorbahn, T. Hermann, M. Misiak, E. Stamou, and M. Steinhauser, Phys. Rev. Lett. **112**, 101801 (2014), 1311.0903.
- [155] A. Abdesselam et al. (Belle), in *Proceedings, 51st Rencontres de Moriond on Electroweak Interactions and Unified Theories: La Thuile, Italy, March 12-19, 2016* (2016), 1603.06711, URL <http://inspirehep.net/record/1431982/files/arXiv:1603.06711.pdf>.
- [156] R. Watanabe, Phys. Lett. B **776**, 5 (2018), 1709.08644.
- [157] R. Alonso, B. Grinstein, and J. Martin Camalich, Phys. Rev. Lett. **118**, 081802 (2017), 1611.06676.
- [158] X.-Q. Li, Y.-D. Yang, and X. Zhang, JHEP **08**, 054 (2016), 1605.09308.
- [159] A. Celis, M. Jung, X.-Q. Li, and A. Pich, Phys. Lett. B **771**, 168 (2017), 1612.07757.
- [160] P. A. Zyla et al. (Particle Data Group), PTEP **2020**, 083C01 (2020).
- [161] P. Ball and R. Zwicky, Phys. Rev. **D71**, 014015 (2005), hep-ph/0406232.
- [162] P. Ball and R. Zwicky, Phys. Rev. **D71**, 014029 (2005), hep-ph/0412079.
- [163] M. Beneke, T. Feldmann, and D. Seidel, Eur. Phys. J. **C41**, 173 (2005), hep-ph/0412400.
- [164] J. A. Bailey et al. (MILC), Phys. Rev. D **92**, 034506 (2015), 1503.07237.
- [165] J. A. Bailey et al. (Fermilab Lattice, MILC), Phys. Rev. D **89**, 114504 (2014), 1403.0635.
- [166] Y. Amhis et al. (Heavy Flavor Averaging Group (HFAG)) (2014), 1412.7515.
- [167] T.-W. Chiu, T.-H. Hsieh, C.-H. Huang, and K. Ogawa (TWQCD), Phys. Lett. **B651**, 171 (2007), 0705.2797.
- [168] A. M. Sirunyan et al. (CMS), Phys. Rev. D **98**, 032005 (2018), 1805.10228.
- [169] S. Sahoo and R. Mohanta, Phys. Rev. D **91**, 094019 (2015), 1501.05193.
- [170] S. Sahoo and R. Mohanta, Phys. Rev. D **93**, 114001 (2016), 1512.04657.
- [171] D. Bečirević, O. Sumensari, and R. Zukanovich Funchal, Eur. Phys. J. **C76**, 134 (2016),

1602.00881.

- [172] J. Charles et al., Phys. Rev. **D91**, 073007 (2015), 1501.05013.
- [173] J. P. Lees et al. (BaBar), Phys. Rev. **D86**, 012004 (2012), 1204.2852.
- [174] R. Aaij et al. (LHCb), Phys. Rev. Lett. **123**, 211801 (2019), 1905.06614.
- [175] W. Altmannshofer et al. (Belle-II), PTEP **2019**, 123C01 (2019), 1808.10567.
- [176] R. Aaij et al. (LHCb) (2018), 1808.08865.
- [177] Y. Miyazaki et al. (Belle), Phys. Lett. **B699**, 251 (2011), 1101.0755.
- [178] B. Bhattacharya, A. Datta, J.-P. Guévin, D. London, and R. Watanabe, JHEP **01**, 015 (2017), 1609.09078.
- [179] D. Bečirević, N. Košnik, O. Sumensari, and R. Zukanovich Funchal, JHEP **11**, 035 (2016), 1608.07583.
- [180] B. Chakraborty, C. T. H. Davies, G. C. Donald, J. Koponen, and G. P. Lepage (HPQCD), Phys. Rev. **D96**, 074502 (2017), 1703.05552.
- [181] T. Hambye, PoS **IDM2010**, 098 (2011), 1012.4587.
- [182] A. Biswas, D. Borah, and D. Nanda, JCAP **09**, 014 (2018), 1806.01876.
- [183] M. Cirelli, N. Fornengo, and A. Strumia, Nucl. Phys. B **753**, 178 (2006), hep-ph/0512090.
- [184] E. Ma and D. Suematsu, Mod. Phys. Lett. A **24**, 583 (2009), 0809.0942.
- [185] A. V. Semenov (1996), hep-ph/9608488.
- [186] A. Pukhov, E. Boos, M. Dubinin, V. Edneral, V. Ilyin, D. Kovalenko, A. Kryukov, V. Savrin, S. Shichanin, and A. Semenov (1999), hep-ph/9908288.
- [187] G. Belanger, F. Boudjema, A. Pukhov, and A. Semenov, Comput. Phys. Commun. **176**, 367 (2007), hep-ph/0607059.
- [188] G. Belanger, F. Boudjema, A. Pukhov, and A. Semenov, Comput. Phys. Commun. **180**, 747 (2009), 0803.2360.
- [189] N. Aghanim et al. (Planck) (2018), 1807.06209.
- [190] Y. Cai and A. P. Spray, JHEP **01**, 087 (2016), 1509.08481.
- [191] X. Cui et al. (PandaX-II), Phys. Rev. Lett. **119**, 181302 (2017), 1708.06917.
- [192] E. Aprile et al. (XENON) (2017), 1705.06655.
- [193] D. S. Akerib et al. (LUX), Phys. Rev. Lett. **118**, 021303 (2017), 1608.07648.
- [194] Z. Bern, P. Gondolo, and M. Perelstein, Phys. Lett. B **411**, 86 (1997), hep-ph/9706538.
- [195] S. Choubey, S. Khan, M. Mitra, and S. Mondal, Eur. Phys. J. C **78**, 302 (2018), 1711.08888.